

(B) Binary pulsars

B.1 : Pulsars

* Highly magnetized neutron star, born from supernova explosion ($5 \rightarrow 10 M_{\odot}$)

$\left\{ \begin{array}{l} \text{mass} \approx 1.4 M_{\odot} \quad (\text{between } 1.2 \text{ and } 2) \\ \text{radius} \approx 10 \text{ km} \quad (\text{depends on Eq. of state} \\ \text{of nuclear matter}) \\ \text{rotation} \approx 1 \text{ to } 30 \text{ times per second} \end{array} \right.$

[cf. 30 times a trip around Paris per second!]

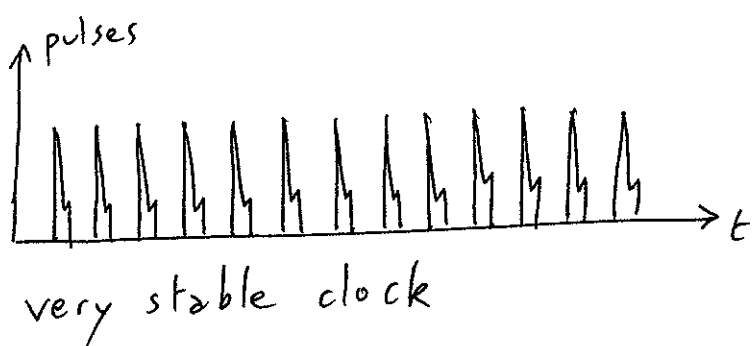
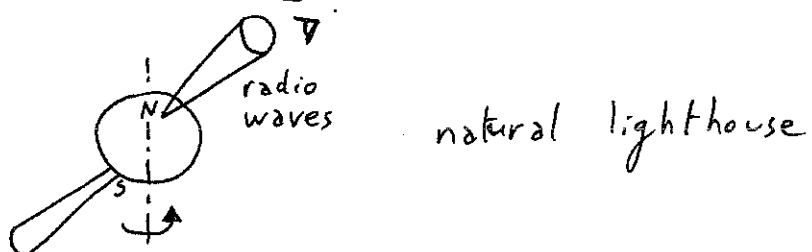
Large gravitational field

$$\boxed{\frac{Gm}{Rc^2} \approx 0.15}$$

large

, as compared to 2×10^{-6} for \odot
and 7×10^{-10} for \oplus

[Maximum = $\frac{1}{2}$ for black holes]



(actually, pulses
are quite noisy,
but obtained by
superposing 10s
of them,

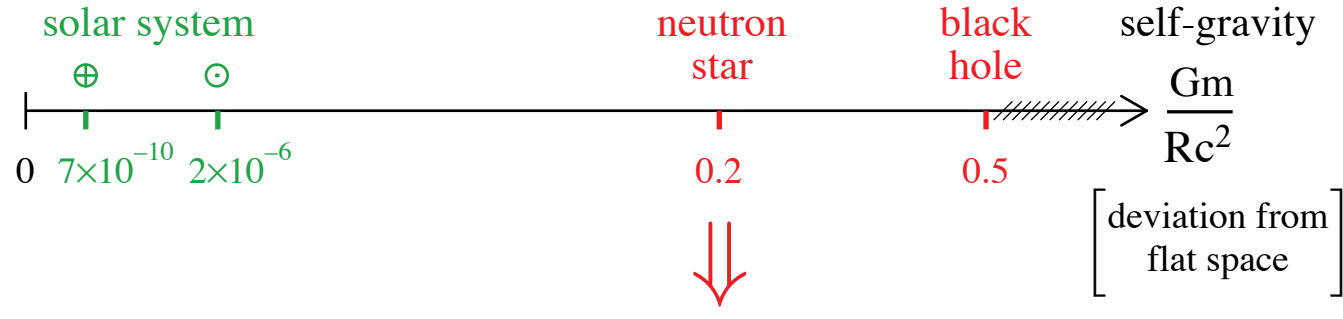
[Nobel prize 1974 for Antony Hewish
[Pulsars discovered by his student Jocelyn Bell.]

Today, we know about 1600 pulsars.

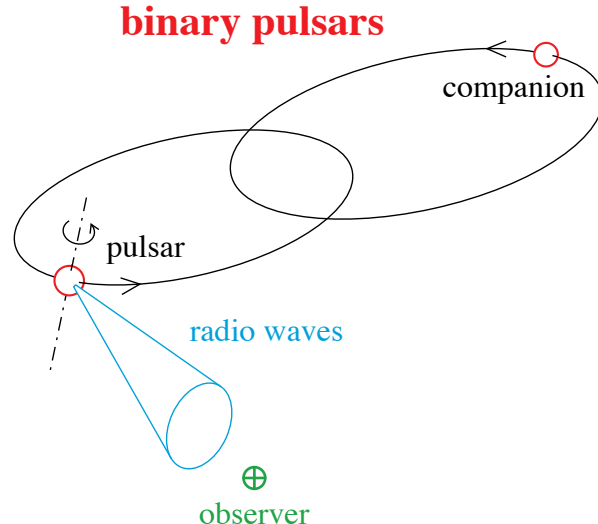
Weak-field experiments

$$\left\{ \begin{array}{l} -g_{00} = 1 - 2 \frac{Gm}{rc^2} + 2 \beta^{\text{PPN}} \left(\frac{Gm}{rc^2} \right)^2 + \dots \\ g_{ij} = \delta_{ij} \left[1 + 2 \gamma^{\text{PPN}} \frac{Gm}{rc^2} + \dots \right] \end{array} \right.$$

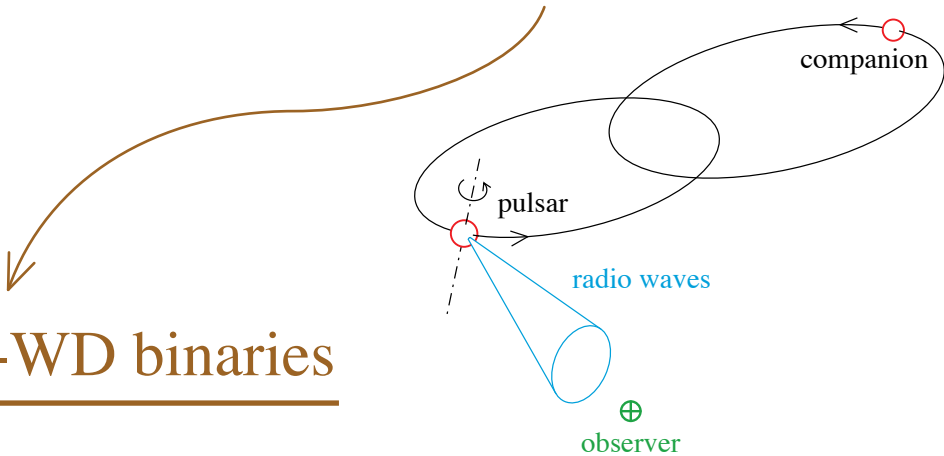
Strong-field tests ?



moving clock
giving information
about this strong-
gravity region



- ~ 1600 known pulsars
- ~ 100 binary pulsars



Many NS-WD binaries

PSR J1141–6545 →
[Kaspi *et al.* 1999]

PSR J0407+1607
PSR J2016+1947
...

PSR J0751+1807 ⇒ 2.1 m_\odot NS!
[Nice *et al.* 2005]

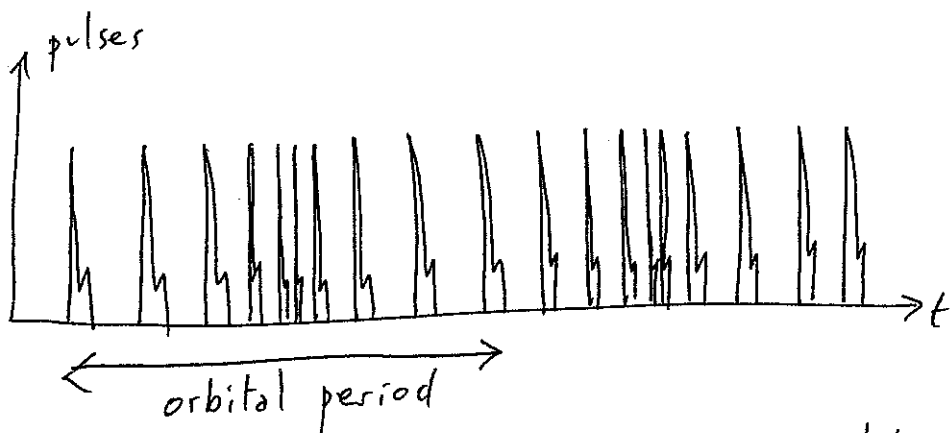
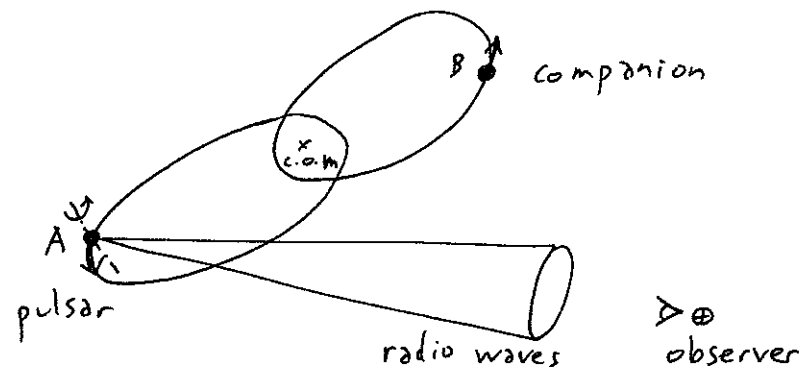
8 NS-NS binaries

{ PSR B1913+16 [Hulse-Taylor 1974]
PSR B1534+12 [Wolszczan 1991]
PSR J0737–3039 [Burgay *et al.* 2003]

PSR B2127+11C (in globular cluster)
PSR J1756–2251 [Faulkner *et al.* 2004]
PSR J1518+4904
PSR J1811–1736
PSR J1829+2456

PSR J1906+07 [Lorimer *et al.* 2005]
(maybe NS-WD?)

* Binary pulsars = pulsar and companion body orbiting around their center of mass.
 = moving clock, the best tool that one could dream of to test a relativistic theory.

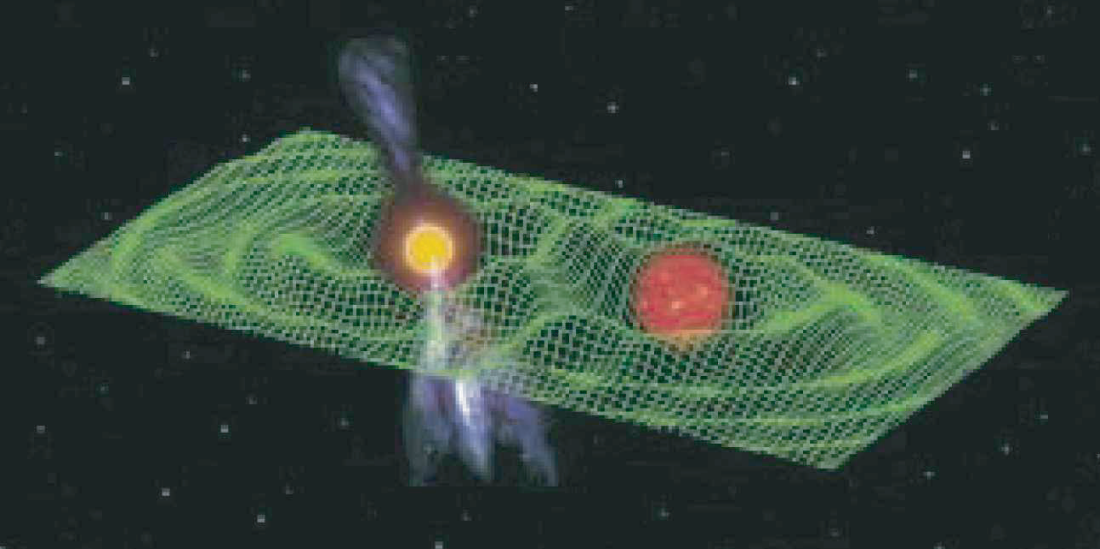


The pulse frequency is modulated by the pulsar's motion, mainly because of the Doppler effect.

⇒ by analyzing the times of arrival, one gets ultra-precise information about the pulsar's orbit (seen in a "stroboscopic" way)

{ Today, we know about 100 binary pulsars, but only few of them have a fast enough orbit to provide measurements of relativistic effects.

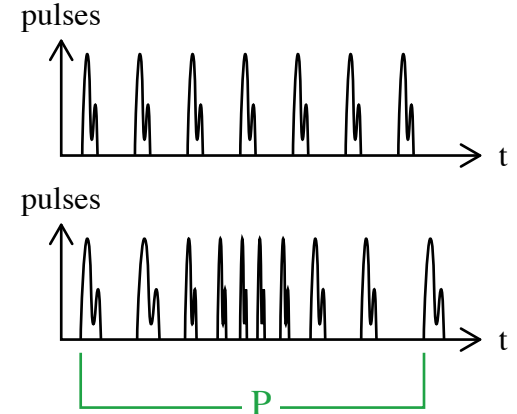
[N.B.: only 9 of these binary pulsars are made of 2 neutron stars. Many of the others are neutron star-white dwarf binaries.]



Binary-pulsar tests

pulsar = (very stable) clock

binary pulsar = moving clock



- Time of flight across orbit $\propto \frac{\text{size of orbit}}{c}$ (“Roemer time delay”)

- orbital period P
 - eccentricity e
 - periastron angular position \square
 - ...
- }
- “Keplerian” parameters

- Redshift $\propto \frac{G m_B}{r_{AB} c^2}$ + second order Doppler effect $\propto \frac{\vec{v}_A^2}{2 c^2}$ (“Einstein time delay”)

- parameter \square_{Timing}

- Time evolution of Keplerian parameters

- periastron advance \square (order $\frac{1}{c^2}$)

- gravitational radiation damping \dot{P} (order $\frac{1}{c^5}$)

- }
- “post-Keplerian” observables
[PSR B1913+16 • Hulse & Taylor]

3	2	= 1
observables	unknown	test
masses m_A, m_B		

Plot the three curves [strips]

$\square_{\text{Timing}}^{\text{theory}}(m_A, m_B) = \square_{\text{Timing}}^{\text{observed}}$	}
$\square^{\text{theory}}(m_A, m_B) = \square^{\text{observed}}$	
$\dot{P}^{\text{theory}}(m_A, m_B) = \dot{P}^{\text{observed}}$	

“ $\square - \square - \dot{P}$ test”

B.2: post-Keplerian formalism

(39)

* Different relativistic (& Newtonian) effects do not have the same time signature. T. Damour has shown in his lectures that the arrival times may be fitted by a "timing formula" [Damour-Deruelle 1986] involving several phenomenological parameters.

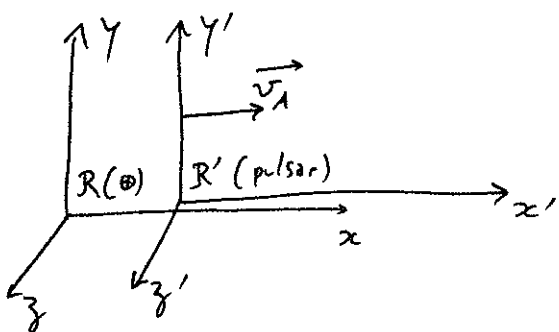
Keplerian parameters	P	orbital period
	T ₀	time of reference
	e ₀	eccentricity
	w ₀	position of periastron (max. of pulse frequency at equal time from 2 minima or not?)
	x ₀ = $\frac{a_A \sin i}{c}$	projection of semi-major axis along line of sight

post-Keplerian parameters	k = $\frac{\langle \dot{\omega} \rangle P}{2\pi}$	periastron advance (and observable periodic effect!)
	γ_{Timing}	Einstein time delay ($\Delta \neq \frac{1}{\sqrt{1-v^2/c^2}}$ but linked $\neq \gamma_{\text{PPN}} \neq \gamma_{\text{AB}}$)
	$\langle \dot{P} \rangle$	orbital period change (due to emission of gravitational waves)
	r, s	range and shape of Shapiro time delay
	$\begin{cases} \delta_0 \\ \dot{e} \\ \dot{x} \end{cases}$	difference between various "eccentricities" time variations of $\{x\}$ (radiation damping & spin-orbit effects)
4 extra parameters which cannot be separated		

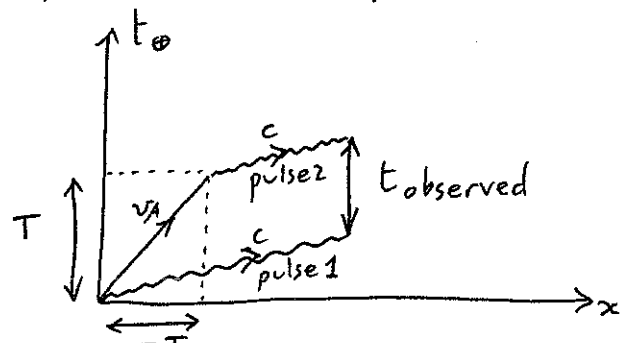
* Instead of re-doing the rigorous analysis of Damour-Dervelle,^(4D)
 let us here merely illustrate the physics involved in
 various terms.

a) Doppler effect

[special relativity]



- If pulsar moves along line of sight



$$\text{Galilean mechanics (absolute time)}: v_A T = c(T - t) \Rightarrow t_{\text{obs}} = (1 - \frac{v_A}{c}) T$$

Special relativity

$$T = \frac{T'_{\text{proper}}}{\sqrt{1 - v_A^2/c^2}}$$

$$\Rightarrow t_{\text{observed}} = \sqrt{\frac{1 - v_A/c}{1 + v_A/c}} T'_{\text{proper}}$$

- IF pulsar moves \perp line of sight, one just gets the special relativistic dilatation of time $t_{\text{obs}} = \frac{T'_{\text{proper}}}{\sqrt{1 - v_A^2/c^2}}$.

- General case

$$t_{\text{observed}} = \frac{1 - \frac{v_A/\text{line of sight}}{c}}{\sqrt{1 - \frac{v_A^2_{\text{total}}}{c^2}}} T'_{\text{proper}}$$

(41)

The main $\frac{1}{c}$ effect allows us to measure the Keplerian parameters quoted above.

b) Einstein time delay

At order $\frac{1}{c^2}$, the second-order Doppler effect is combined with the variable redshift caused by the companion (at a varying distance from the pulsar if the orbit is elliptic).

$$\begin{aligned} c d\tau'_{\text{proper}} &= \sqrt{-g_{\mu\nu} dz_A^\mu dz_A^\nu} \quad \xleftarrow{\text{pulsar's worldline}} \\ &= \sqrt{-g_{00} c dT c dT - 2 g_{0i} c dT dz_A^i - g_{ij} dz_A^i dz_A^j} \\ &\quad \uparrow \qquad \qquad \qquad \uparrow O\left(\frac{1}{c^3}\right) \qquad \uparrow \\ &\quad 1 - \frac{2 G m_B}{r_{ABC} c^2} + \text{const.} + O\left(\frac{1}{c^4}\right) \qquad \qquad \qquad \delta_{ij} + O\left(\frac{1}{c^2}\right) \\ &= \sqrt{1 - \frac{2 G m_B}{r_{ABC} c^2} + \text{const.} - \frac{\vec{v}_A^2}{c^2} + O\left(\frac{1}{c^4}\right)} c dT \end{aligned}$$

$$\Rightarrow T'_{\text{proper}} \times \left(1 + \frac{G m_B}{r_{ABC} c^2} + \text{const.} + \frac{\vec{v}_A^2}{2 c^2} + O\left(\frac{1}{c^4}\right) \right) \times \left(1 - \frac{v_A}{c} \right) = t_{\text{observed}}$$

\uparrow
 Einstein effect
 (grav. redshift)

\uparrow
 cf. the special
 relativistic
 time dilation

\uparrow
 Doppler standard

For a Keplerian orbit

$$\left\{ \begin{array}{l} \vec{r} = \frac{a(1-e^2)}{1+e\cos\theta} \begin{pmatrix} \cos\theta \\ \sin\theta \end{pmatrix} \quad (\text{for reduced mass}) \\ \vec{v} = \sqrt{\frac{GM}{a(1-e^2)}} \begin{pmatrix} -\sin\theta \\ e+\cos\theta \end{pmatrix} \end{array} \right.$$

$$\begin{aligned} \frac{G m_B}{r_{ABC} c^2} + \frac{\vec{v}_A^2}{2 c^2} &= \frac{G m_B (1+e\cos\theta)}{a(1-e^2) c^2} + \frac{1}{2 c^2} \left(\frac{m_B}{m_A+m_B} \right)^2 \frac{G(m_A+m_B)}{a(1-e^2)} [1+e^2+2e\cos\theta] \\ &= \text{const.} + \left(\frac{G m_B}{a c^2} e \left[1 + \frac{m_B}{m_A+m_B} \right] \right) \frac{\cos\theta}{1-e^2} \quad \text{time dependence} \end{aligned}$$

One defines

$$\frac{2\pi}{P} \times \gamma_{\text{Timing}} = \frac{G m_B}{a c^2} e \left[1 + \frac{m_B}{m_A + m_B} \right] \quad (42)$$

in G.R.

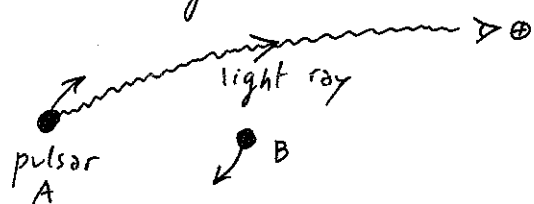
extractible from timing data
because of $\cos\theta \Rightarrow \exists$ time dependence

in scalar-tensor theories

$$\left[1 + \frac{m_B}{m_A + m_B} (1 + \alpha_A \alpha_B) - \alpha_B \frac{\partial \ln I_A}{\partial \varphi_0} \right]$$

involves the variation of the pulsar's inertia moment
due to the varying background φ_0 caused by the companion
(\Rightarrow change of equilibrium configuration).

c) Shapiro time delay



$$\text{Null geodesic } d\tilde{s}^2 = ds^2 = 0 \Rightarrow dt \simeq \frac{|d\vec{x}|}{c} \left(1 + \frac{2Gm_B}{c^2 r_B} + \text{const. in time} + O\left(\frac{1}{c^4}\right) \right)$$

$$\Rightarrow \int_{t_{\text{emission}}}^{t_{\text{arrival}}} dt \simeq \frac{1}{c} \int_{t_e}^{t_a} |d\vec{x}| + \frac{2}{c^3} \int_{t_e}^{t_a} \frac{G m_B}{|\vec{x} - \vec{r}_B|} |d\vec{x}|$$

(take into account
motion of observer
between t_e and t_a !)

Logarithmic effect derived in
C. Will's lectures, where $\vec{z}_B(t)$
moves on a Keplerian ellipse at 1st order.

In timing formula, with the angle $u - \text{esin}u = \frac{2\pi}{P}(T' - T_0)$ defined in
Damour's lectures, one gets

$$t_{\text{observed}} = \dots \quad [\text{previous expression p. (41)}]$$

$$- 2 \left(\frac{G m_B}{c^3} \right) \ln \left\{ 1 - e \cos u - \frac{S_{\text{ini}}}{\sin u} \left[\sin u (\cos u - e) + \sqrt{1 - e^2} \cos u \sin u \right] \right\}$$

"range" (4) "shape" (5)

d) Periastron advance

(43)

$$P_x \langle \dot{\omega} \rangle = \frac{6\pi G_{AB}(m_A + m_B)}{c(1-e^2)c^2} \times \left[\frac{1 - \frac{1}{3}\alpha_A\alpha_B}{1 + \alpha_A\alpha_B} - \frac{m_A\alpha_A^2\beta_B + m_B\alpha_B^2\beta_A}{6(m_A + m_B)(1 + \alpha_A\alpha_B)^2} \right]$$

cf. $\frac{2\gamma^{PPN} - \beta^{PPN} + 2}{3}$ in Will's

lectures on PPN formalism.

e) Orbital period change : cf. expressions p. (36)

B.3: PSRs B1913+16 & B1534+12

* PSR B1913+16 (position on sky : 19h 13 min; 16°)

Discovered in 1974 by Hulse & Taylor [Nobel prize 1993].

- Period $P = 27906.97958755(35)s \approx 7h45\text{ min}$ (quick!)
- Projected semi-major axis $\frac{a_A \sin i}{c} = 2.3417725(8)s$ (small!)
- [we know from post-Keplerian analysis that $i \approx 47^\circ \Rightarrow a_A \approx 3.2s$
 $\approx 2 \times \oplus - \odot$]
- Eccentricity $e = 0.6171338(4)$ (large)

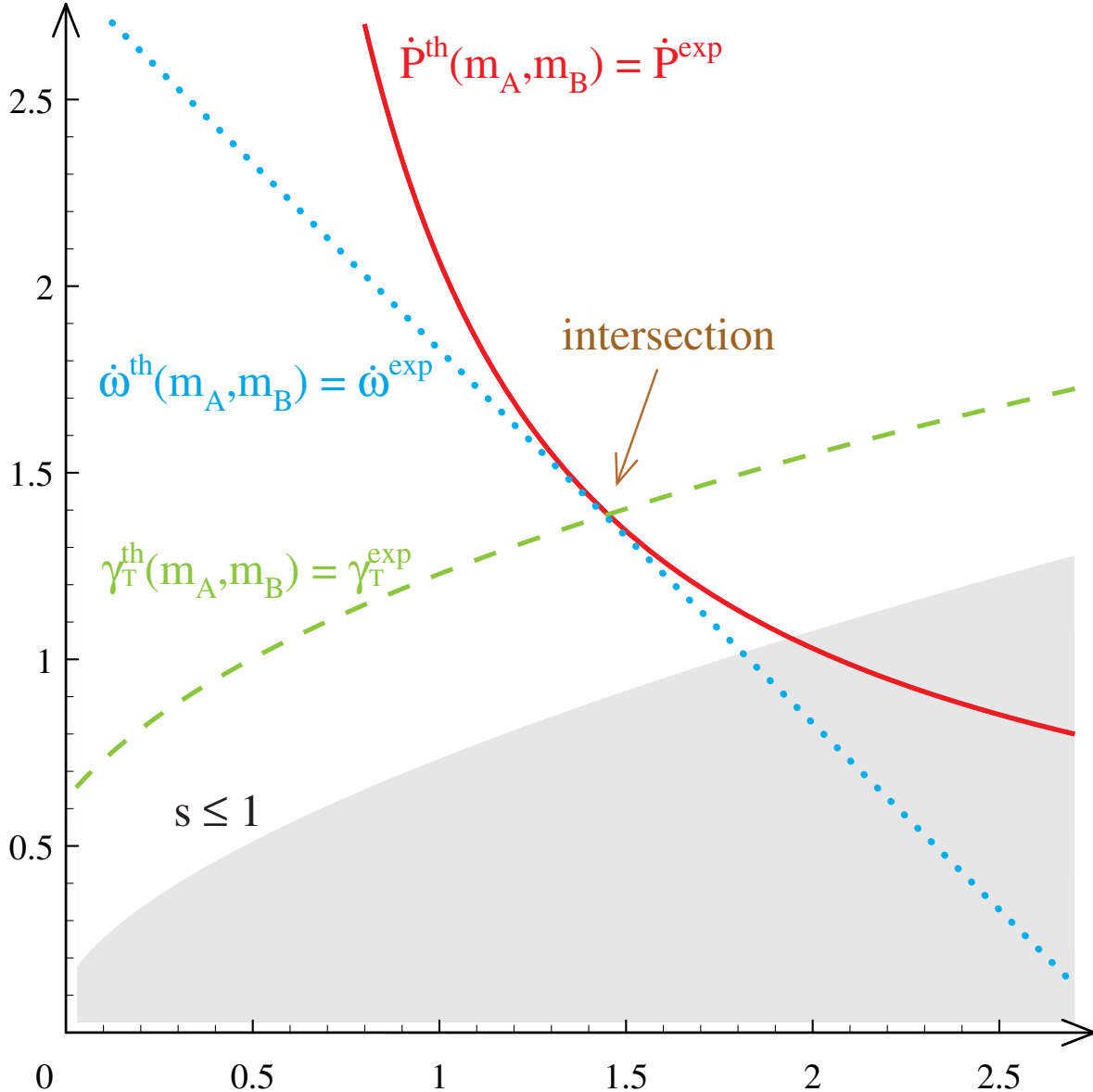
Observed post-Keplerian parameters:

$$\left\{ \begin{array}{l} \gamma_{\text{Timing}}^{\text{obs}} = 4.2919(8) \text{ ms} \\ \langle \dot{\omega} \rangle^{\text{obs}} = 4.226595(5)^\circ \text{ yr}^{-1} \text{ (cf. } 43''/\text{century for } \gamma!) \\ \langle \dot{P}^{\text{obs}} \rangle = -2.4184(9) \times 10^{-12} \text{ (no unit)} \\ \qquad \qquad \qquad \text{several digits on a } 10^{-12} \text{ effect} \Delta \end{array} \right.$$

PSR B1913+16
in general relativity

companion

m_B/m_\odot

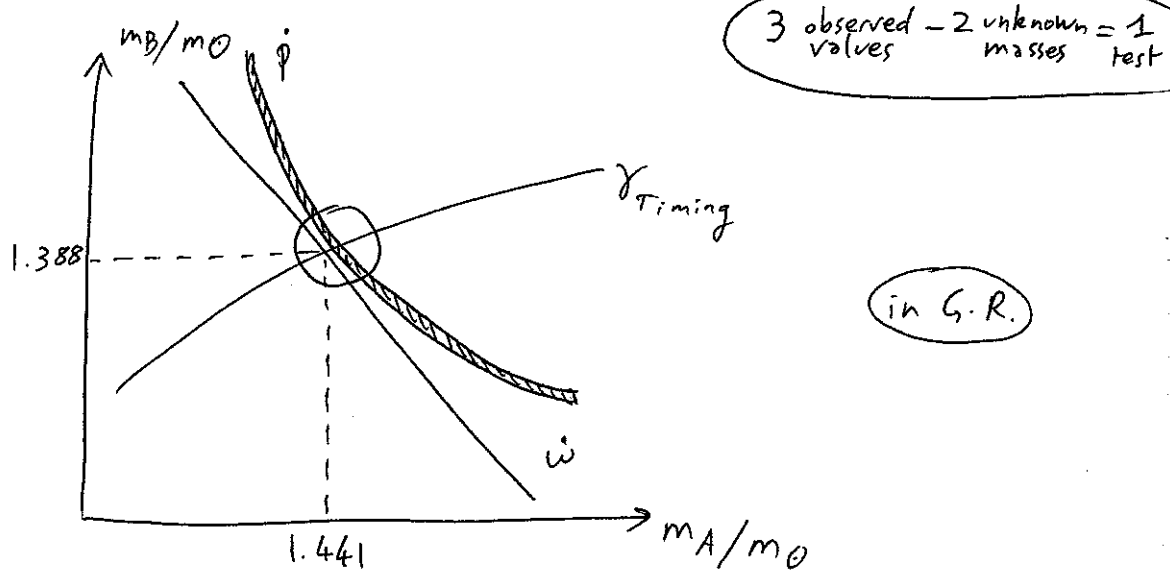


Discovered by R. Hulse and J. Taylor in 1974

$$\begin{aligned}\dot{\omega} &= 4.22661^\circ/\text{yr} \\ \gamma_T &= 4.294 \text{ ms} \\ \dot{P} &= -2.421 \times 10^{-12} \end{aligned} \xrightarrow{\text{GR}} \begin{aligned}m_A &= 1.4408 m_\odot \\ m_B &= 1.3873 m_\odot\end{aligned}$$

In any theory of gravity (say G.R., tensor-scalar),
 one predicts these post-Keplerian parameters in terms
 of the Keplerian ones and the unknown masses (m_A , m_B). (44)

⇒ plot predictions(m_A, m_B) = observed values



The \dot{p} (thin) strip is inconsistent by 18 standard deviations
 from the intersection of the w and γ lines !!!
 (Note that the w and \dot{p} curves suffice to exhibit an inconsistency,
 without any need for γ_T !)

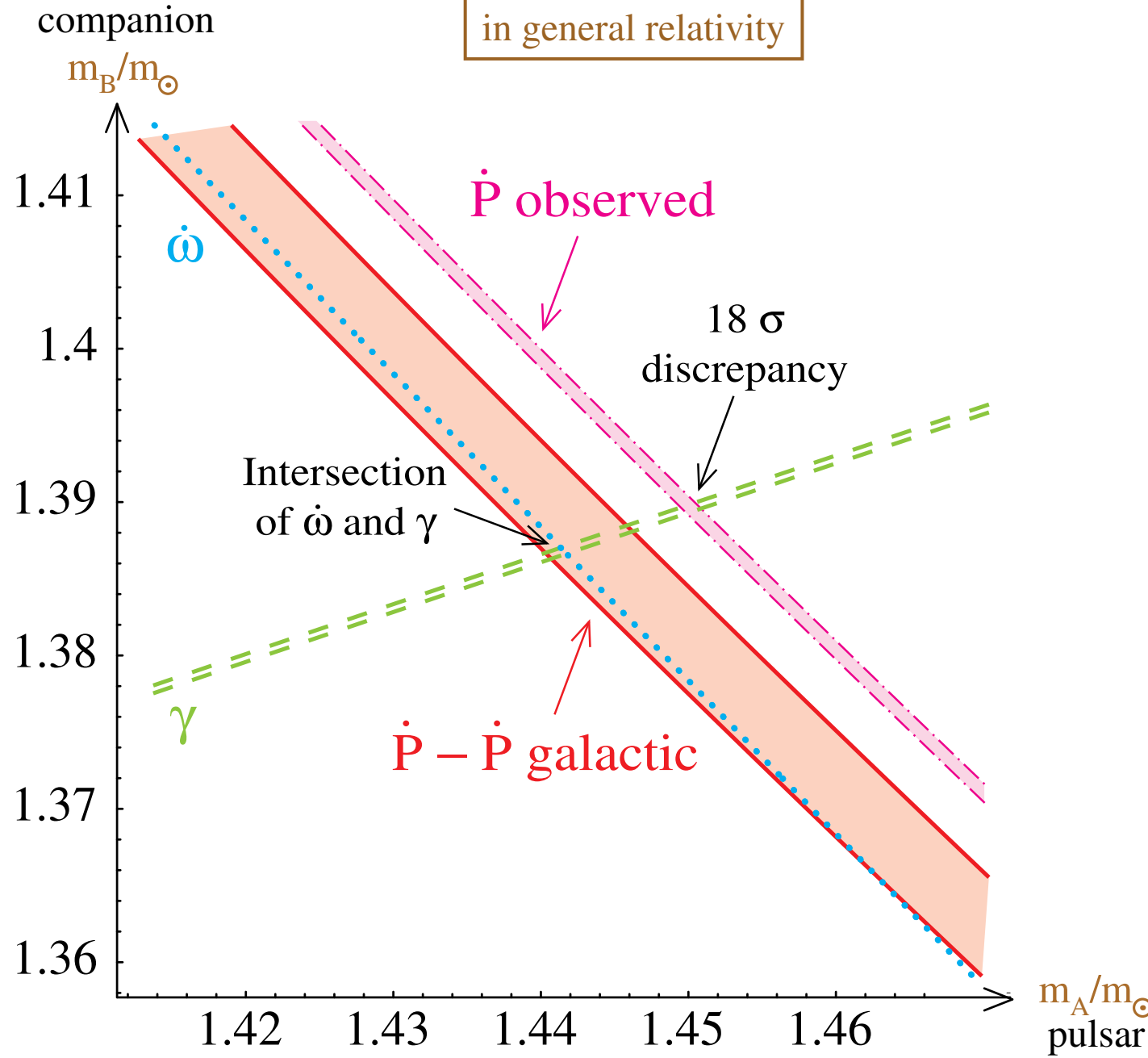
No, because \exists variable Doppler effect contributing to
 measured \dot{p} , due to acceleration of system towards
 center of galaxy. [Damour & Taylor 1991]

$$\text{Doppler} \approx \vec{n} \cdot \vec{v}$$

$(\vec{n}: \text{unit vector from } \oplus \text{ to pulsar})$

$$\Rightarrow \frac{d \text{Doppler}}{dt} \approx \vec{n} \cdot \vec{a} + \frac{v^2}{d_{\oplus-\text{PSR}}} \quad \begin{array}{l} \uparrow \\ \text{relative acceleration} \\ \text{towards Galaxy's} \\ \text{center} \end{array} \quad \begin{array}{l} \downarrow \\ \text{Shklovskii effect} \\ (\text{larger when pulsar is close!}) \end{array}$$

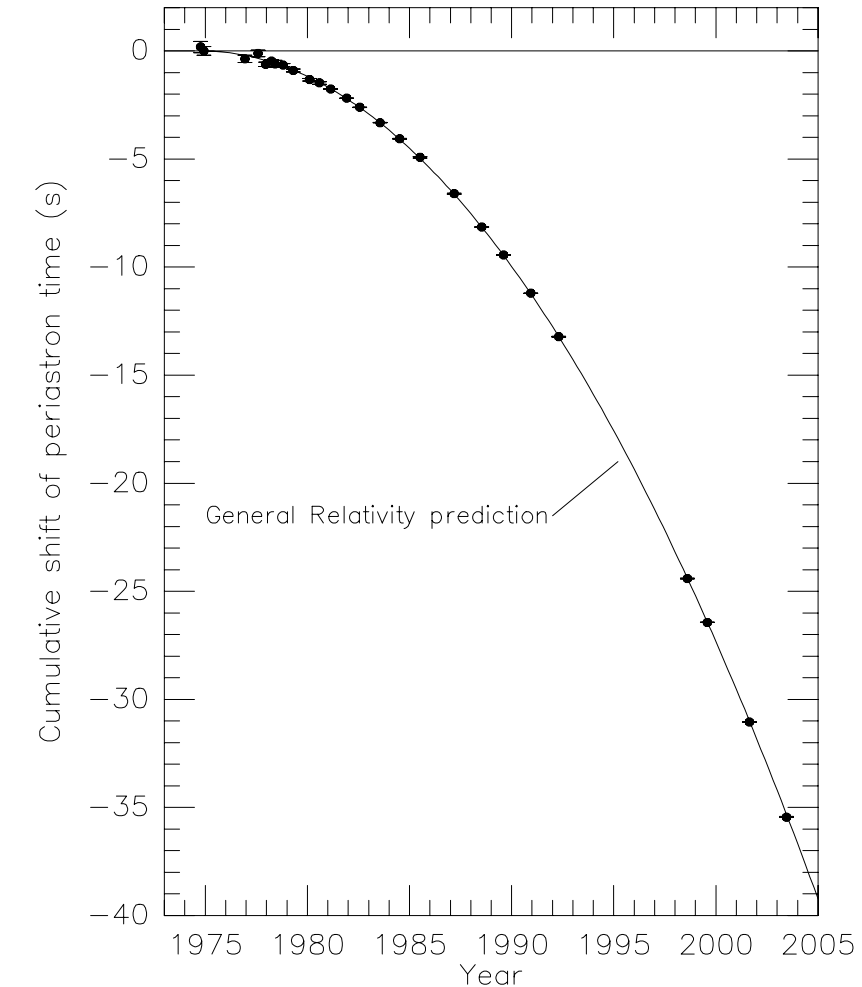
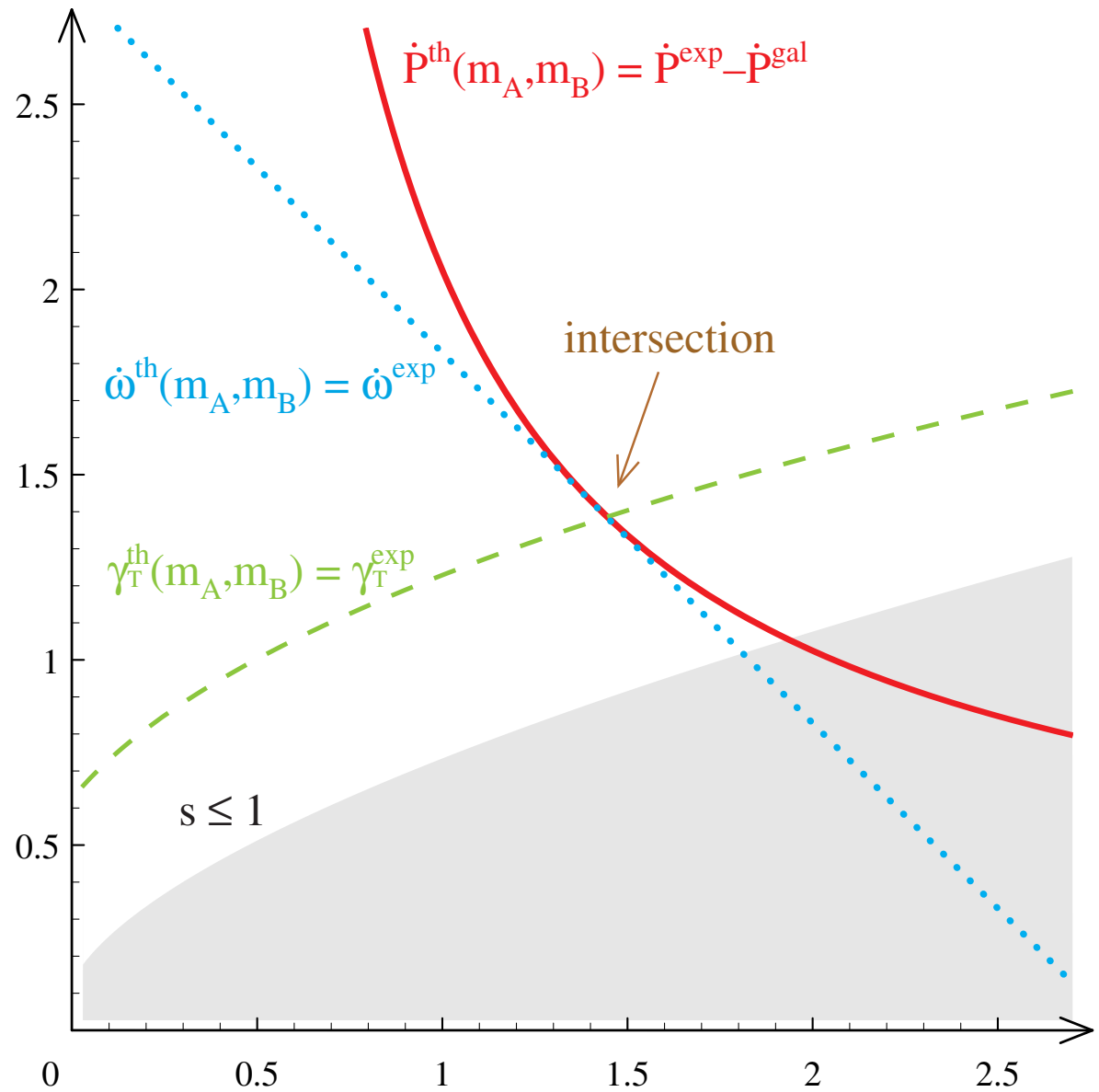
PSR B1913+16
in general relativity



companion

$$m_B/m_\odot$$

PSR B1913+16
in general relativity



$$\begin{aligned}\dot{\omega} &= 4.22661^\circ/\text{yr} \\ \gamma_T &= 4.294 \text{ ms} \\ \dot{P} &= -2.421 \times 10^{-12} \end{aligned} \quad \xrightarrow{\text{GR}} \quad \begin{aligned}m_A &= 1.4408 m_\odot \\ m_B &= 1.3873 m_\odot\end{aligned}$$

Discovered by R. Hulse and J. Taylor in 1974

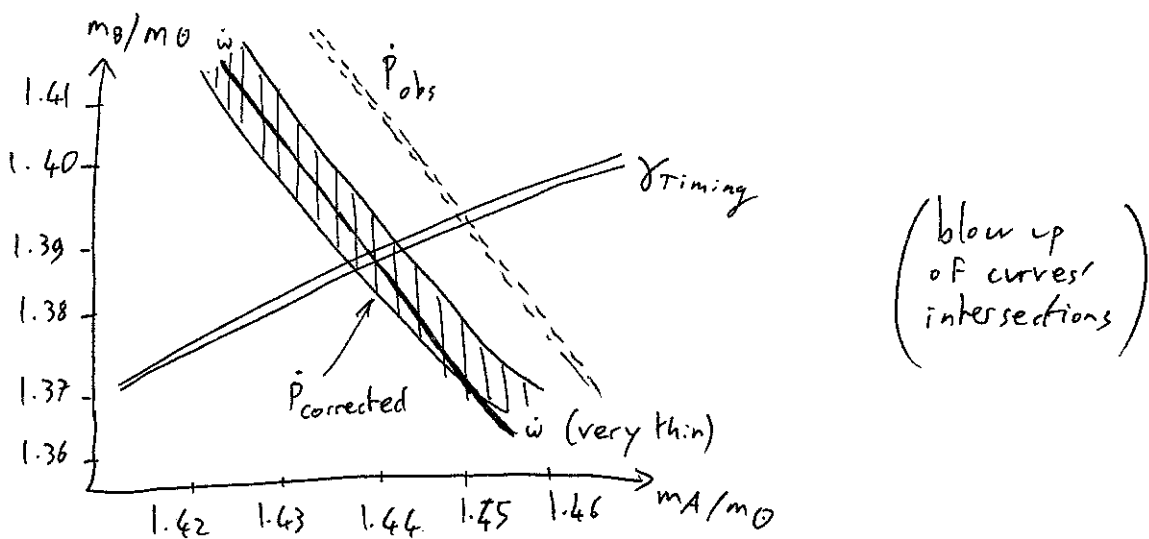
(45)

$\Rightarrow \dot{P}_{obs}$ should be corrected by $-\dot{P}_{gal}$ to be compared with $\dot{P}_{predicted}(m_A, m_B)$:

$$\left. \begin{aligned} \dot{P}_{gal} &= -0.0128(50) \times 10^{-12} \\ \dot{P}_{corrected} = \dot{P}_{obs} - \dot{P}_{gal} &= -2.4056(51) \times 10^{-12} \end{aligned} \right\}$$

↑
errors dominated
by \dot{P}_{gal} , unfortunately

but now the central value is
consistent (at better than 1σ)
with G.R.'s predictions [for
 m_A, m_B deduced from ω & γ_{Timing}].

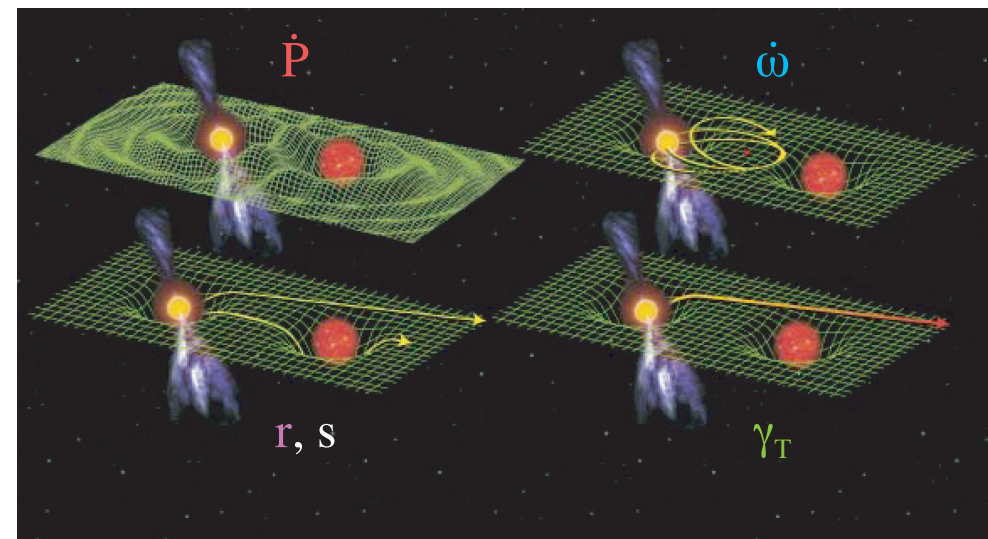
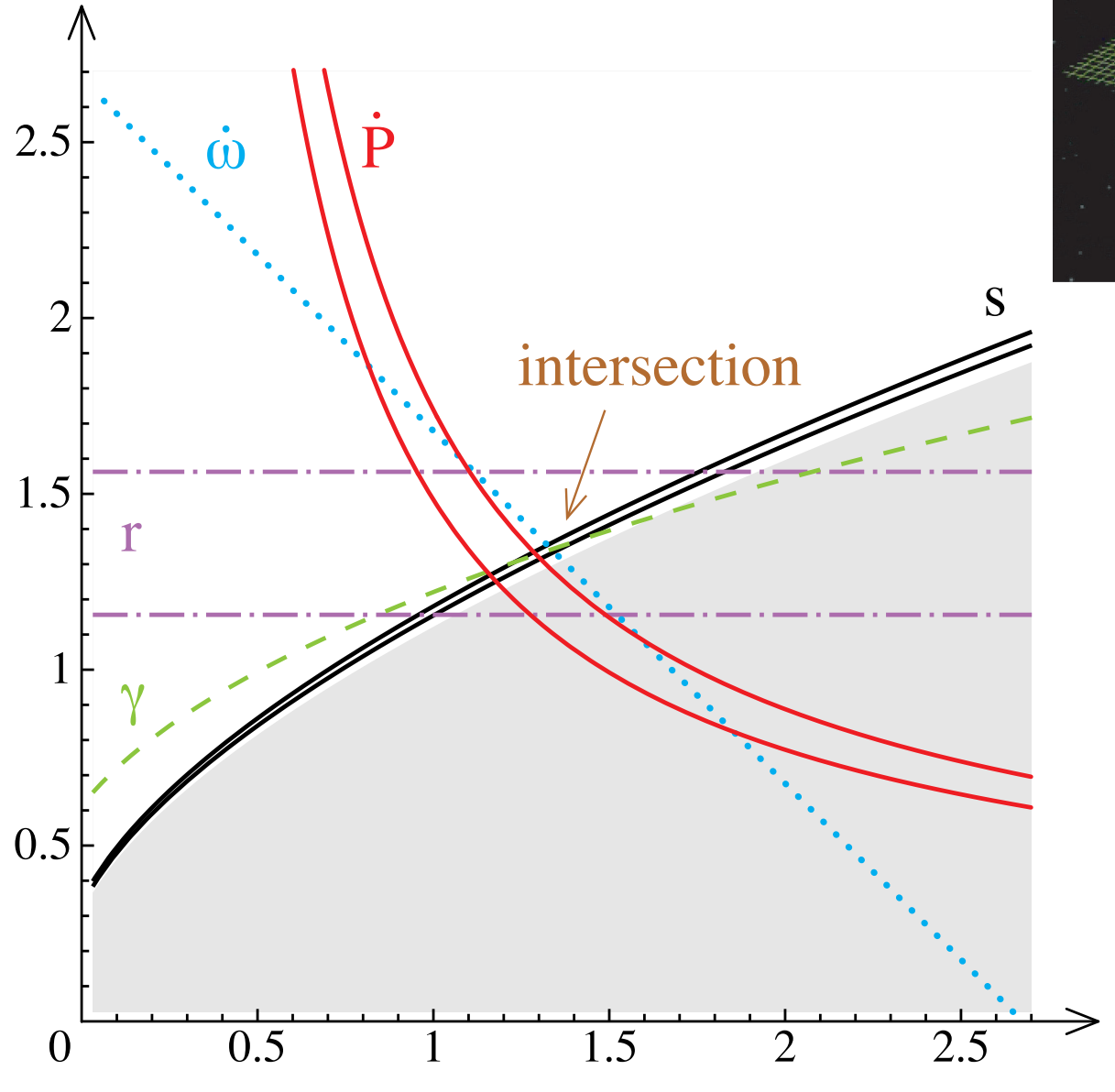


$$\boxed{\frac{\dot{P}_{obs} - \dot{P}_{gal}}{\dot{P}_{G.R.}}} = 1.0013 \pm 0.0021 \quad \text{in G.R.}$$

precision < 3% for effect of order 10^{-12} Δ

companion
 m_B/m_\odot

PSR B1534+12
 in general relativity



5 observables \square 2 masses = 3 tests

“Galactic” contribution to \dot{P}

[Damour–Taylor 1991]

$$\text{Doppler} \propto n.v \quad \frac{d \text{ Doppler}}{d t} \propto n.a + \frac{v^2}{d_{\text{OPSR}}}$$

*PSR B1534+12

Discovered by A. Wolszczan in 1991. Timing: I. Stairs' thesis.

- Closer to earth : $d_{\text{PSR}} \sim 1 \text{ kpc}$ (as compared to $\sim 6 \text{ kpc}$ for 1913+16)
 - \Rightarrow brighter
- ⊕ bonuses
 - Pulses narrower \Rightarrow less noise
 - orbit seen almost from edge : $i = 79^\circ$ (as compared to $\approx 77^\circ$ for 1913+16)
 - \Rightarrow relativistic effects more visible
notably the Shapiro time delay (r, s)
 - 
- drawbacks
 - But slightly slower orbit $P_b \approx 10 \text{ h}$ (as compared to $7 \text{ h } 45 \text{ min}$ for 1913+16)
 - [size $r_{AB}/c \approx 8 \text{ s}$ as compared to $\approx 6 \text{ s}$ for 1913+16]
 - \Rightarrow slightly smaller relativistic effects,
e.g. $\langle \omega \rangle \approx 1.76^\circ \text{ yr}^{-1}$ (as compared to $4.2^\circ \text{ yr}^{-1}$ for 1913+16)
 - Smaller eccentricity $e \approx 0.27$ (as compared to 0.62 for 1913+16)
 - \Rightarrow smaller Einstein time delay, for instance
 $\gamma_T \approx 2 \text{ ms}$ (as compared to 4.3 ms for 1913+16)
 - Slightly smaller neutron star masses : $m_A = 1.33 m_\odot$, $m_B = 1.35 m_\odot$
(deduced from observed PK parameters in G.R.) (as compared to 1.44 and 1.39 for 1913+16)
 - \Rightarrow slightly less constraining for scalar-tensor theories,
 - But GREAT interest of this system is that it provides us with the measure of 5 PPK parameters : $\gamma_T, \omega, \dot{\rho}, r, s$

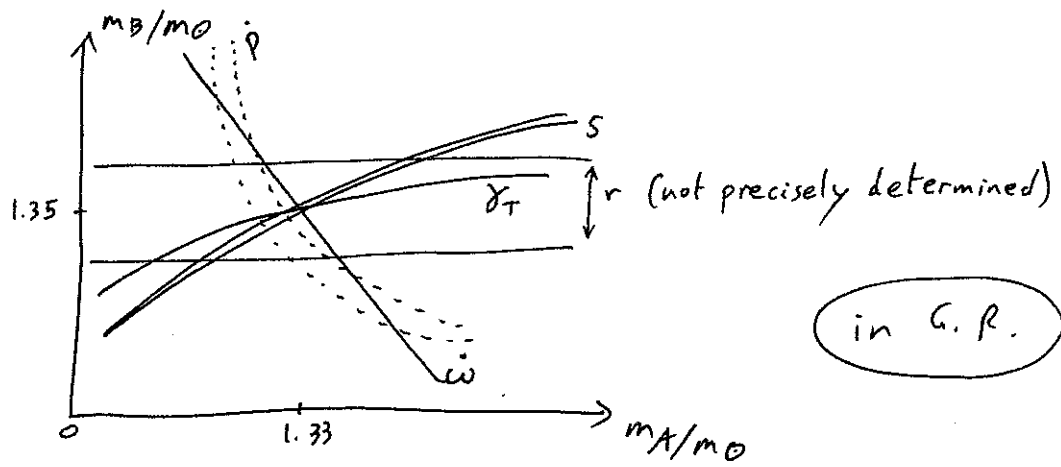
$$\Rightarrow 5 - 2 = 3 \text{ tests}$$

unknown masses

One of these tests, intersection of the 3 thin strips $[\gamma_T, \omega, s]$ in the (m_A, m_B) plane, gives a test of strong-field gravity independent of the radiative structure ($\dot{\rho}$) :

$$\frac{s^{\text{obs}}}{s^{\text{G.R.}} (m_A, m_B \text{ deduced from } \gamma_T, \omega)} = 1.000 \pm 0.007$$

(1% level)



⚡ Problem: even when taking into account the "galactic" contribution to \dot{p} , the corrected \dot{p} is not consistent with the intersection of the 4 other strips, at the 1.7σ level. This is because the Shklovskii contribution depends crucially on our estimate of d_{PSR} , from dispersion measurements (i.e., the fact that ≠ frequencies reach the observer at slightly ≠ times, because of the gas of e^- which is crossed on the path). Actually, we know today that our distance estimates from dispersion were too large (many pulsars should have been located exactly on the boundary of the Galaxy!) \Rightarrow a ^{more} recent model makes this \dot{p} consistent with all ^{other} 4 observed PPK parameters. This underlines anyway that the error on \dot{p} is larger than the above width of the strip indicates \Rightarrow \dot{p} cannot be used safely for this close binary pulsar.

* N.B.: Independently of the measured PPK parameters, there is a constraint on the Keplerian ones from Kepler's third law

$$\text{"n}^2 \text{a}^3 = GM" : \left(\frac{2\pi}{P}\right)^2 a^3 = G(M_A + M_B)$$

\Rightarrow "Mass Function"

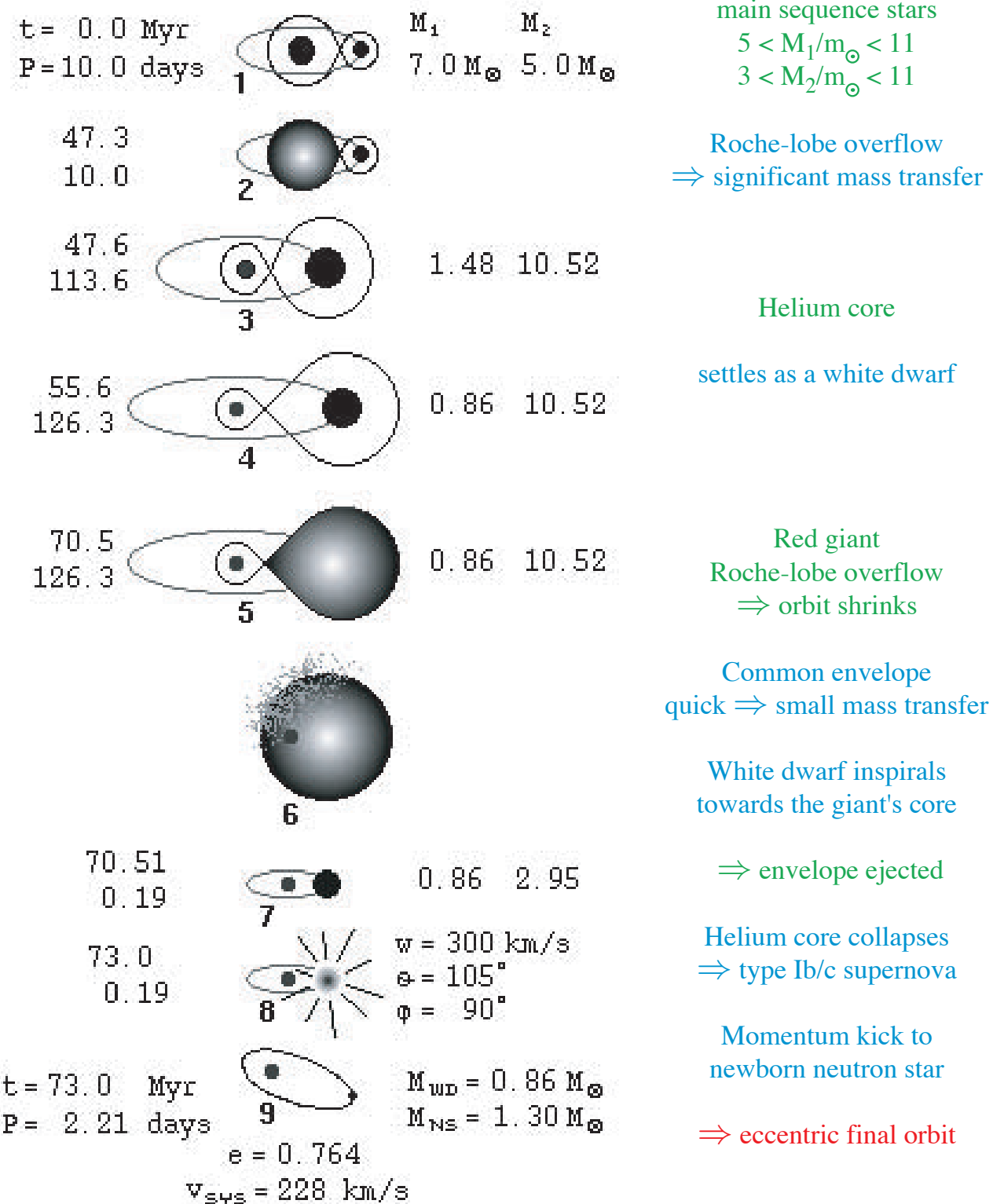
$$\frac{(M_B \sin i)^3}{(M_A + M_B)^2} = \left(\frac{2\pi}{P}\right)^2 \frac{(x c)^3}{G}$$

at lowest (Keplerian) order

Since we know that $|\sin i| \leq 1$, this implies that a region of the mass plane (m_A, m_B) is excluded. Because $s = \sin i \approx 1$ here (orbit seen \approx from edge), it is close to the intersection of the 5 strips, but consistent.

Formation of PSR J1141–6545: neutron star born *after* the white dwarf

[Tauris & Sennels 2000]



B. 4.: The dissymmetric PSR J1141-6545

(48)

Discovered by Kaspi et al. in 1999. Timed by Bailes et al. 2003

- Fast orbit $P \approx 4h45\text{min}$ (cf. $7h45$ for 1913+16)
[size of orbit $S_{AB}/c \approx 4\text{s}$, cf. 6s for 1913+16] \Rightarrow large $\omega = 5.3^\circ \text{yr}^{-1}$
- Rather far from Earth $d_{\oplus-\text{PSR}} > 4\text{kpc}$ (6kpc for 1913+16)
 \Rightarrow expected low Shklovskii correction to P
- Dissymmetric Neutron-star / White dwarf system



$$m_B \approx 0.99 M_\odot$$



- Eccentricity $e \approx 0.17$ large for such a dissymmetric system! $\Rightarrow \omega$ measurable
- Almost seen from edge: $i \approx 76^\circ$ estimate from scintillation measurements, consistent with timing data (unprecise).

- "Slowly" rotating pulsar $P_{\text{PSR}} \approx 400\text{ ms}$ (as compared to 59 ms for 1913+16 and 38 ms for 1534+12), because it is "non-recycled"

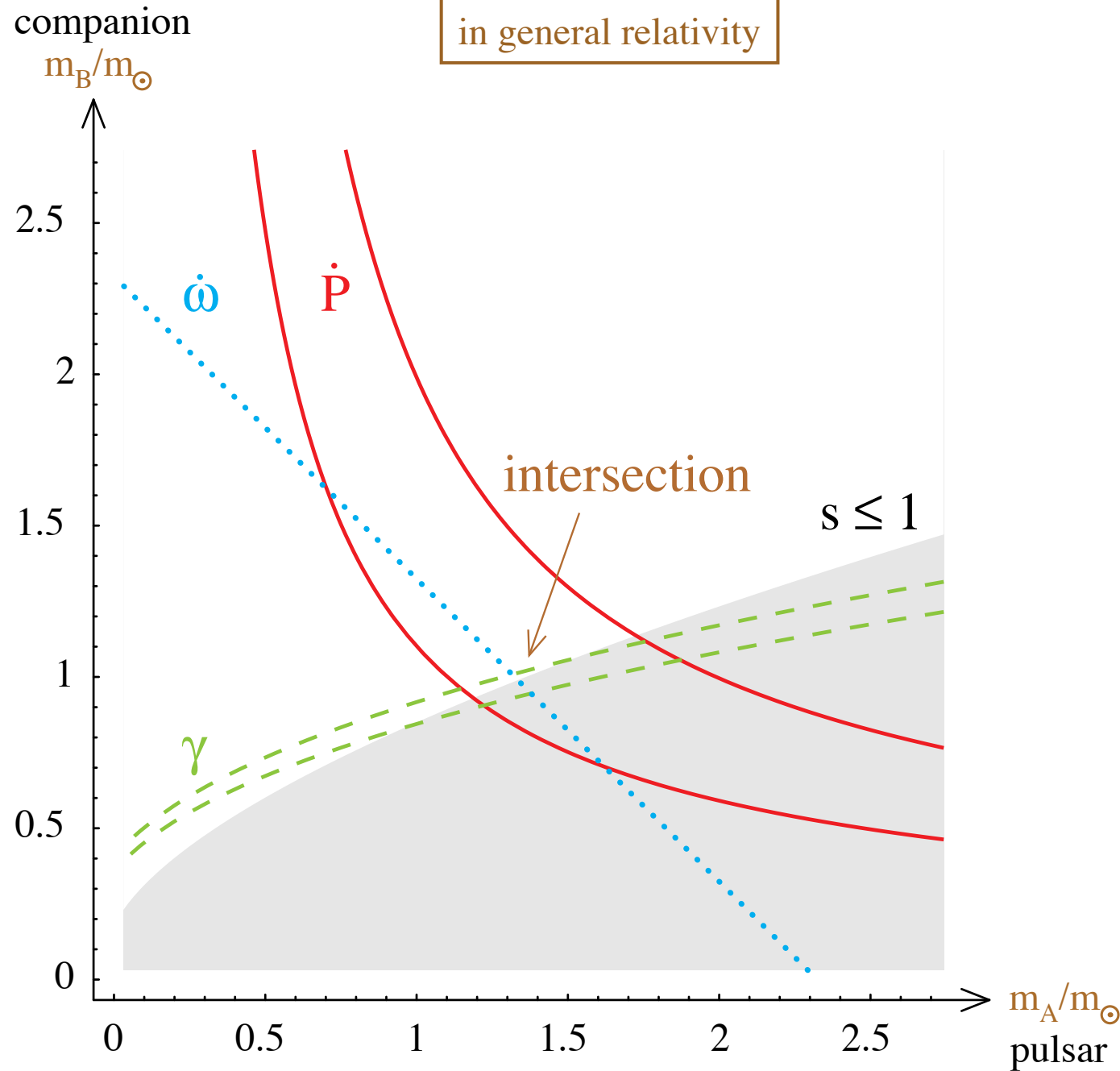
[Formation scenario: neutron star born after the white dwarf (unusual!), cf. [Tauris & Sennels 2000] \Rightarrow newborn NS receives a kick from the SNIb/c explosion \Rightarrow explains the rather large final eccentricity

[whereas we know 10's of NS-WD binaries with vanishingly small e]

(* "Recycled pulsar" = old neutron star which has accreted matter from a companion (before it becomes a compact object itself) \Rightarrow increased spin = best "clocks".

- 3 "red noise" (noise at very low frequencies) because difficult to disentangle real \dot{P} due to gravitational radiation damping from variations of pulse structure due to precession.

PSR J1141–6545
in general relativity

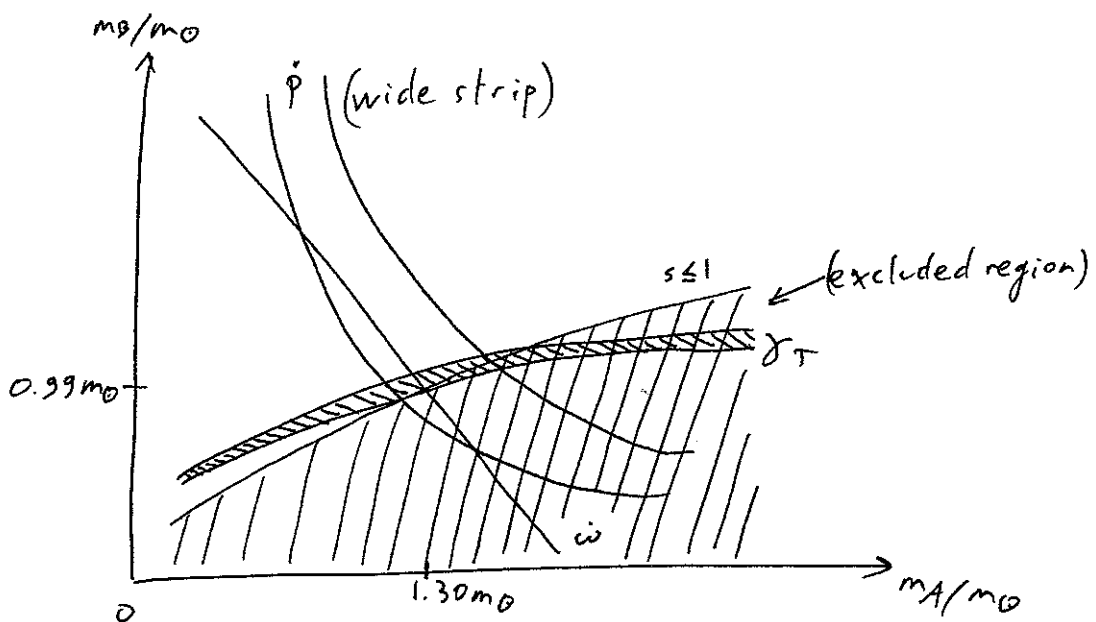


Asymmetrical system
neutron star – **white dwarf**
Neutron star born *after* white dwarf
⇒ eccentricity $e = 0.17$ large
and nonrecycled pulsar

$$\dot{P} = -4 \times 10^{-13}$$

Mass function

$$\frac{(m_B \sin i)^3}{(m_A + m_B)^2} = \left(\frac{2\pi}{P}\right)^2 \frac{(Xc)^3}{G}$$



Consistent with G.R., but test only at the $\sim 25\%$ level.

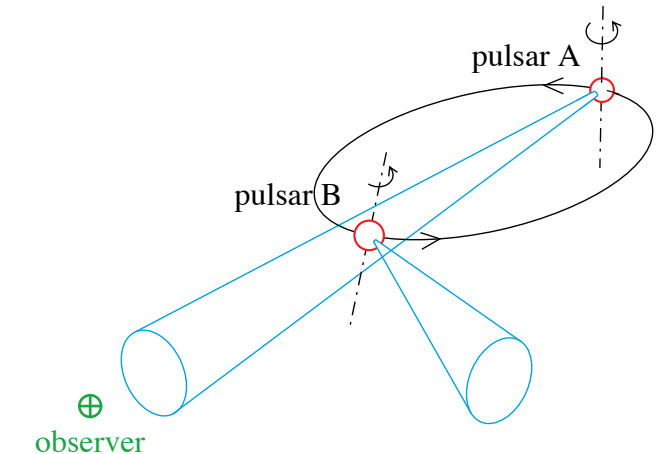
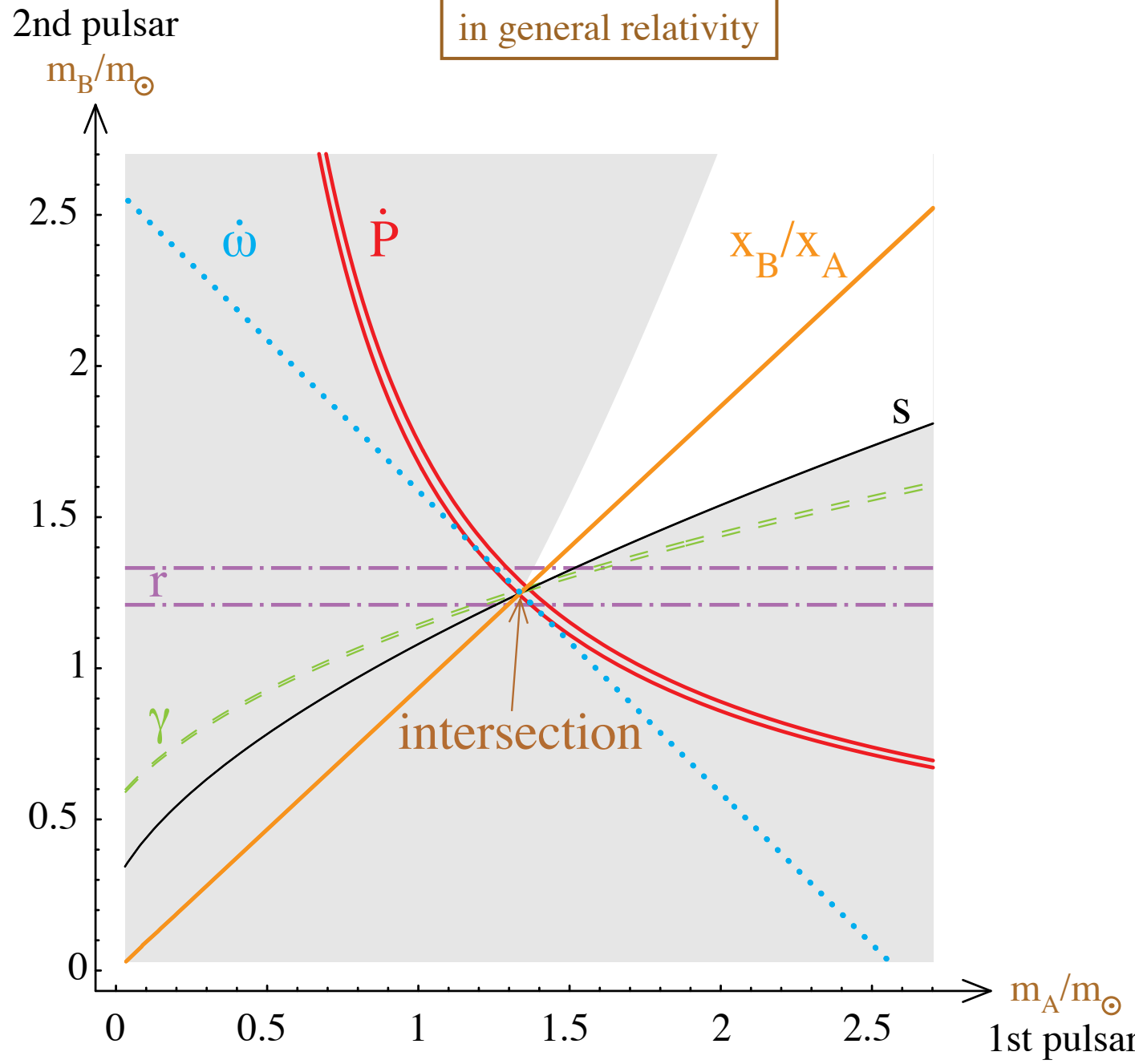
B.6. : The double pulsar PSR J0737-3039

Timing Burgay et al. 2003. Double pulsar Lyne et al. 2004
Most recent data & analysis: M. Kramer et al., Science 2006.

- Very fast orbit : $P = 2 \text{ h } 27 \text{ min } 14.5350 \text{ s}$ $\left[\frac{r_{AB}}{c} \approx 35 \right]$
 $\approx 2x \oplus - \odot$
 - ⇒ more than 1 orbit seen per observation
 - ⇒ large relativistic effects [will merge in 85 Myr as compared to 300 Myr for 1913+16]
 - For instance $\omega = 16.90^\circ \text{ yr}^{-1}$ (cf. $43''/\text{century}$ for \odot
was determined in a few days and 4° yr^{-1} for 1913+16
of observation Δ)
- + • close to the \oplus : $d_{\oplus-\text{PSR}} \approx 0.6 \text{ kpc}$ (10x closer than 1913+16)
[and Shklovskii effect can be estimated rather well]
[because v_I can be extracted from timing data!]
- • Orbit nearly edge-on once more : $i \approx 87^\circ$
• Pulsar's spin // orbit momentum \Rightarrow no precession^(*) & clear signal.
- • Rather small eccentricity $e \approx 0.088$, but enough to measure ω without any problem

^(*) It has been possible to prove so quickly that the pulsar's spin is // orbit's momentum because the period of geodetic precession is $\approx 70 \text{ yr}$ only for this system (very fast, cf. 300 yr for 1913+16 and 700 yr for 1534+12) \Rightarrow no effect observed implies such an alignment.

PSR J0737–3039
in general relativity



$$P = 2 \text{ h } 27 \text{ min } 14.5350 \text{ s}$$

$$\square = 16.90^\circ/\text{yr}$$

$$\frac{x_B}{x_A} = \frac{m_A}{m_B} = 1.07$$

6 observables \square 2 masses = 4 tests

* BEST feature of this system: both neutron stars are detected as pulsars!

(50)

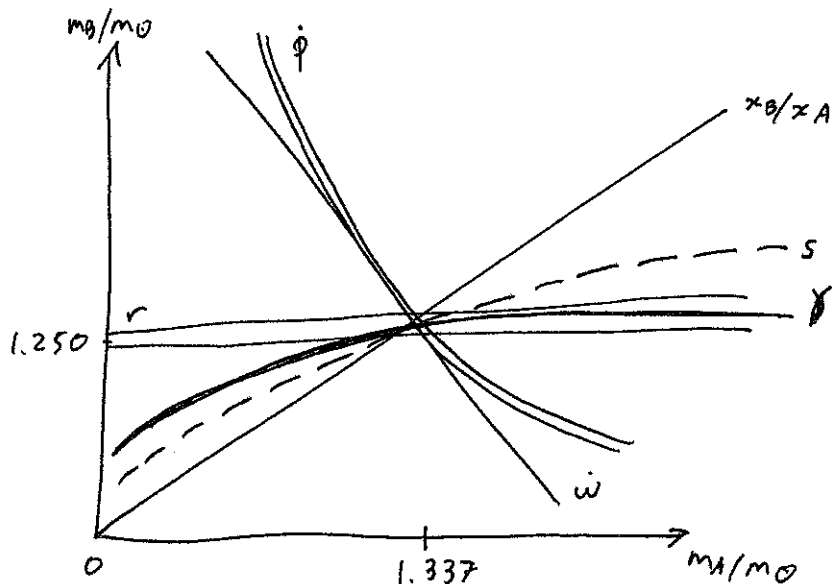
[One is recycled $P_{PSRA} = 23$ ms, but obviously not the other one $P_{PSRB} = 2.8$ s = very slow.]

- 3 eclipses of pulsar A and modulations of B's pulses at A's frequency \Rightarrow probe pulsar magnetospheres.
- Timing of PSR B gives measures of its Keplerian parameters (too noisy for the post-Keplerian), and notably of its projected semimajor axis $\frac{q_B \sin i}{c} = x_B$.

$$\Rightarrow \text{direct measure of } \frac{x_B}{x_A} = \frac{m_A}{m_B} = 1.07$$

This is an extra-constraint in the mass plane $(m_A/m_\odot, m_B/m_\odot)$, in addition to r_T, ω, r, s and $\dot{\phi}$ which have also been measured

$\Rightarrow 6 - 2 = \boxed{4}$ tests of strong-field gravity with this only system Δ



{ + constraints from "mass function" (both for A & B), which exclude most of the mass plane (since $\sin i \approx 1$), but the intersection is consistent with them.

(51)

N.B.: Damour & Taylor [Phys. Rev. D 45 (1992) 1840] have shown that

8 PPK parameters } may be independently
+ 11 pulse-structure ones } measured for each
binary pulsar

$$= 19 - \underbrace{2}_{\text{unknown masses}} - \underbrace{2}_{\text{spin direction}} = (15) \text{ possible tests with each binary pulsar!}$$

At present, we have $\begin{matrix} 1 + 3 \\ 1 \\ 1913+16 \end{matrix} + \begin{matrix} 1 \\ 1 \\ 1534+12 \end{matrix} + \begin{matrix} 4 \\ 1 \\ 1141-6545 \end{matrix} = \underline{\underline{9 \text{ tests}}} \begin{matrix} \\ \\ 0737-3039 \end{matrix}$

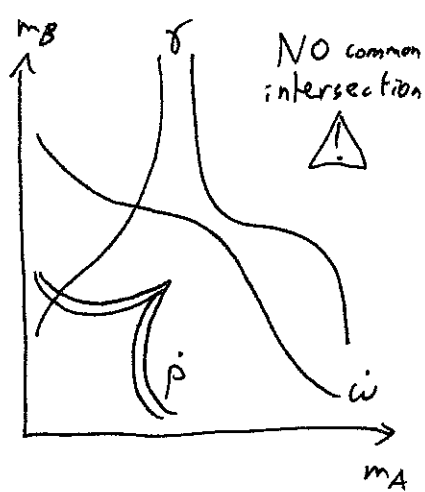
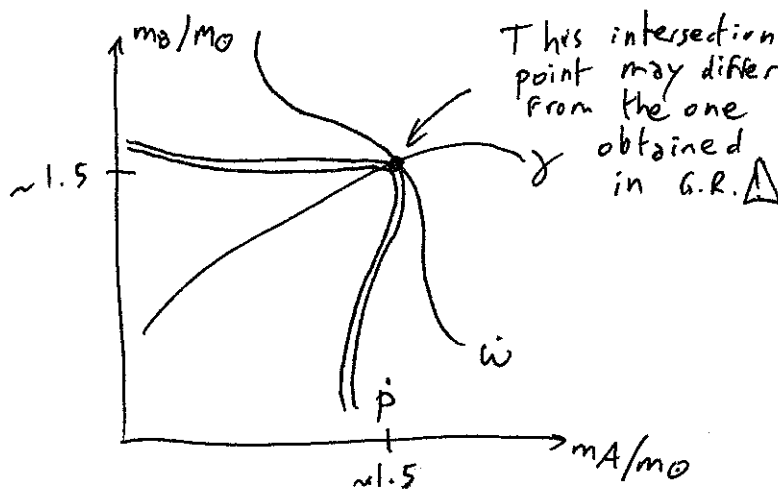
with 4 \neq binary pulsars. \exists other tests (less clean), that we will see in § B.8 below.

B.6: Constraints on scalar-tensor theories

* As seen in § A.7. above, all post-Keplerian parameters are predicted in scalar-tensor theories, and they can thus be compared with experimental data.

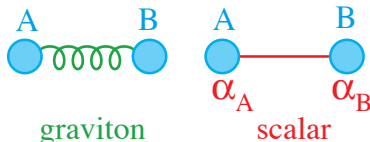
One finds that some theories pass the tests although they can differ significantly from G.R.

and that other theories are merely ruled out

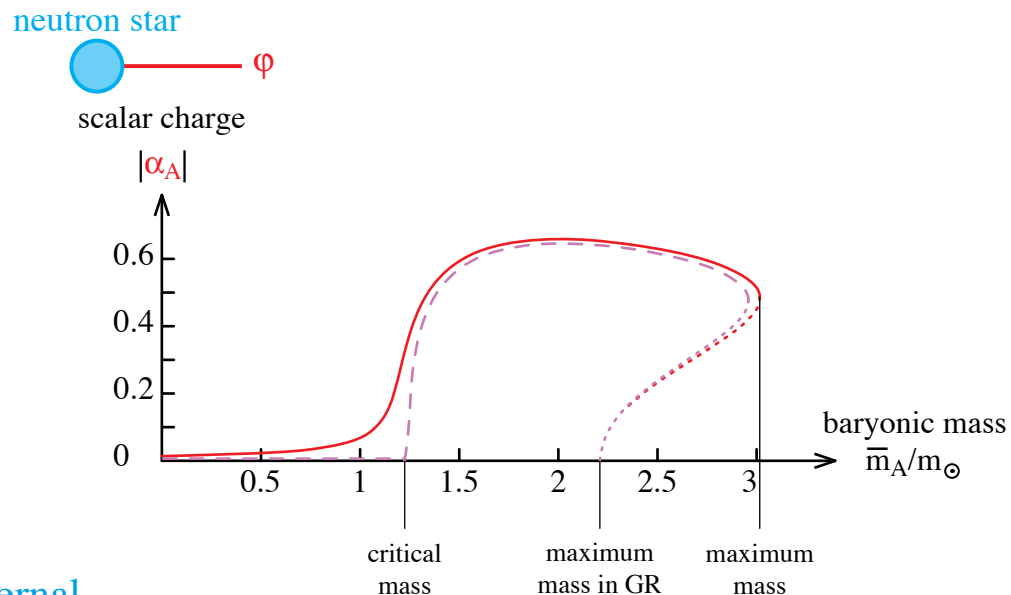


Strong-field effects

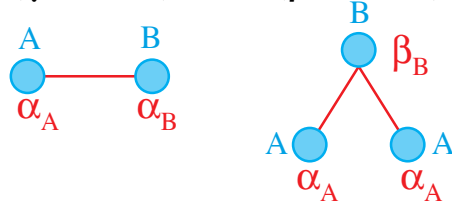
- $G_{AB}^{\text{eff}} = G (1 + \alpha_A \alpha_B)$



depends on internal
structure of bodies A & B



- Similarly for $(\gamma^{\text{PPN}} - 1)$ and $(\beta^{\text{PPN}} - 1) \Rightarrow$ all post-Newtonian effects

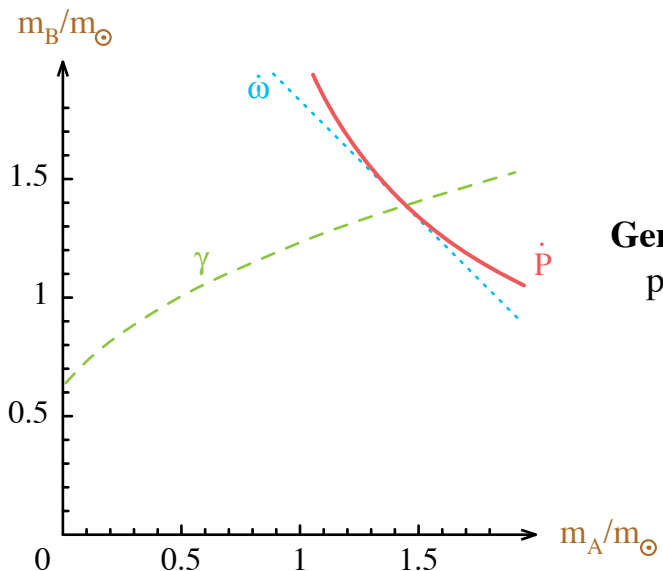


- Energy flux = $\frac{\text{Quadrupole}}{c^5} + O\left(\frac{1}{c^7}\right)$ spin 2

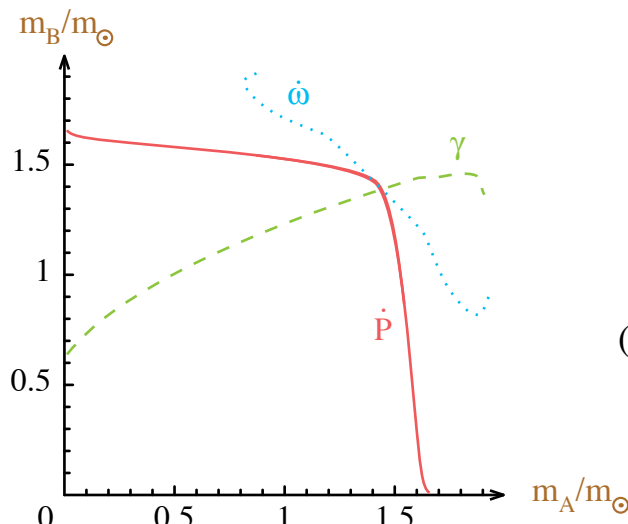
$$+ \frac{\text{Monopole}}{c} \left(0 + \frac{1}{c^2}\right)^2 + \frac{\text{Dipole}}{c^3} + \frac{\text{Quadrupole}}{c^5} + O\left(\frac{1}{c^7}\right) \text{ spin 0}$$

$$\propto (\alpha_A - \alpha_B)^2$$

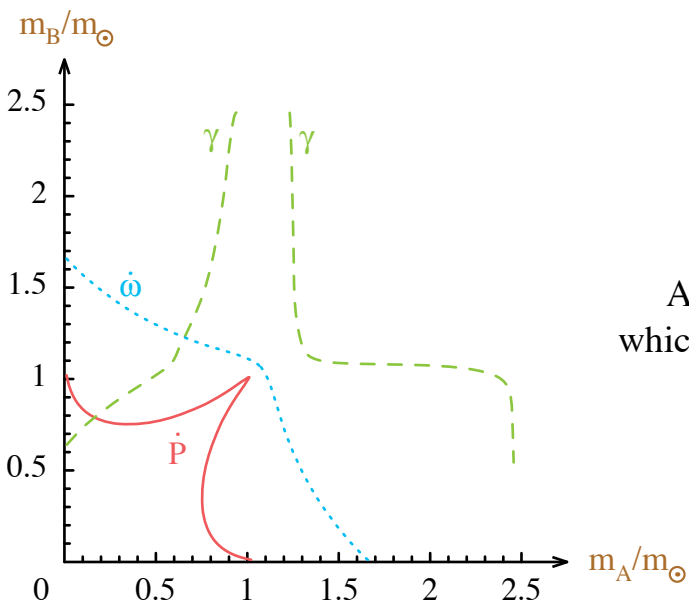
PSR B1913+16
in scalar-tensor theories



General relativity
passes the test

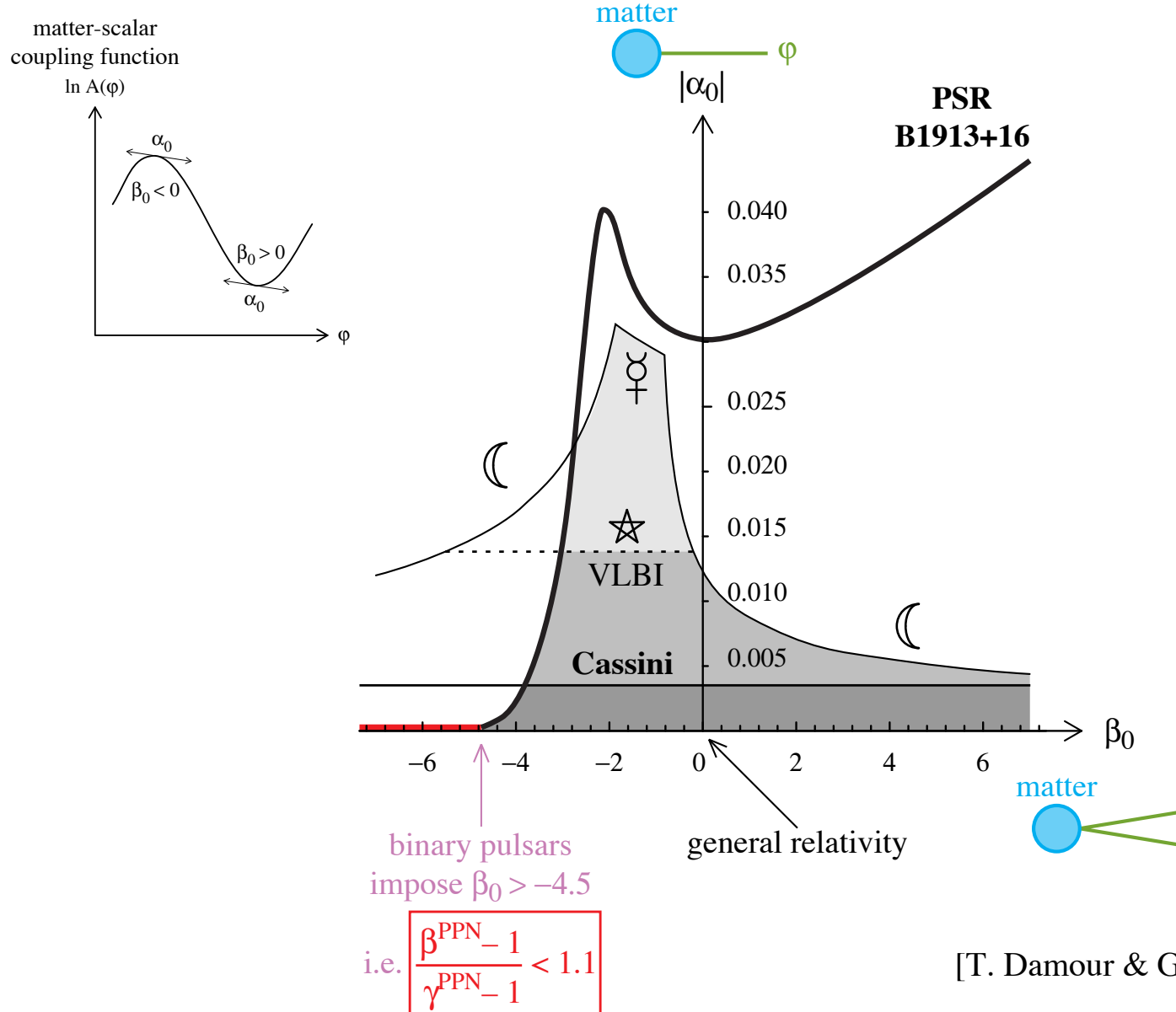


A tensor–scalar theory
which **passes the test**
($\beta_0 = -4.5$, α_0 small enough)



A tensor–scalar theory
which **does not pass the test**
($\beta_0 = -6$, any α_0)

Solar-system & PSR B1913+16 constraints on scalar-tensor theories of gravity



Vertical axis ($\beta_0 = 0$) : Jordan–Fierz–Brans–Dicke theory $\alpha_0^2 = \frac{1}{2 \omega_{\text{BD}} + 3}$

Horizontal axis ($\alpha_0 = 0$) : perturbatively equivalent to G.R.

* One may easily compute the predictions of scalar-tensor theories for any matter scalar coupling function (52)

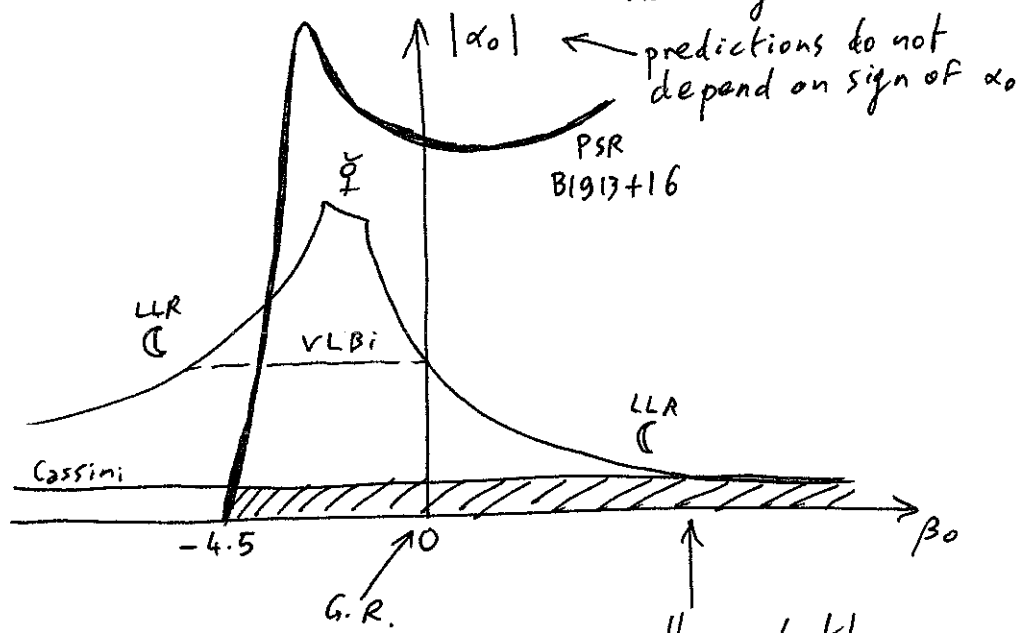
$$\ln \frac{A(\varphi)}{A(\varphi_0)} = \alpha_0 \varphi + \frac{1}{2} \beta_0 \varphi^2 + \frac{1}{3!} \beta_0' \varphi^3 + \dots$$

However, in order to compare binary-pulsar constraints with solar-system ones, it is convenient to restrict the plots to a 2-dimensional space of theories

(≠ "mass planes" plotted above ▲)

$$\boxed{\ln A(\varphi) = \alpha_0 \varphi + \frac{1}{2} \beta_0 \varphi^2}$$

↑ nothing else

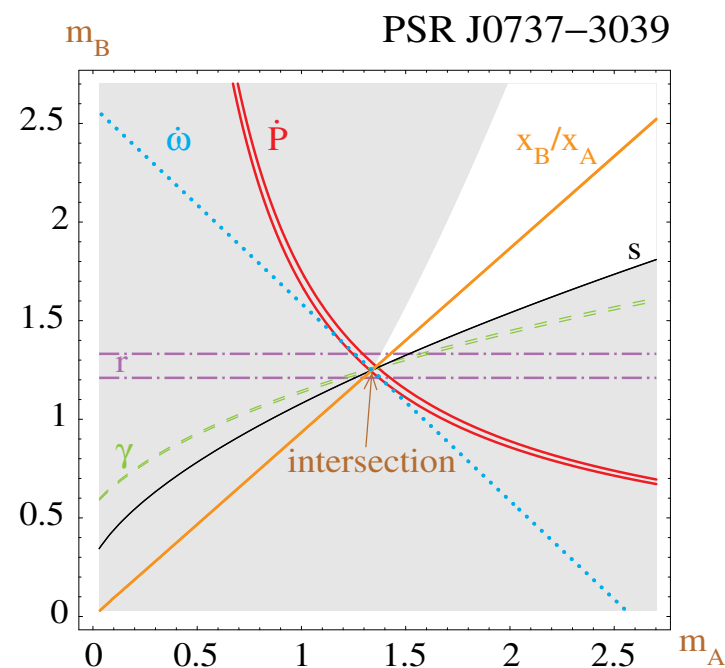
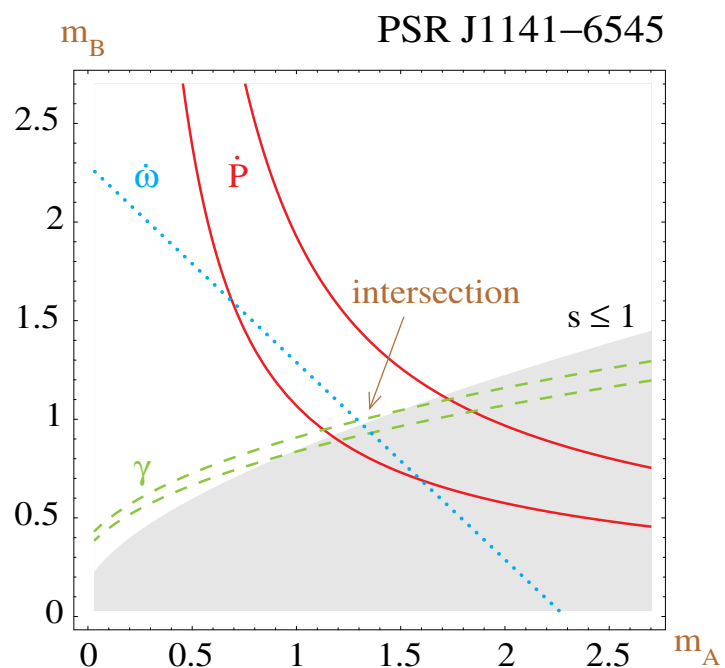
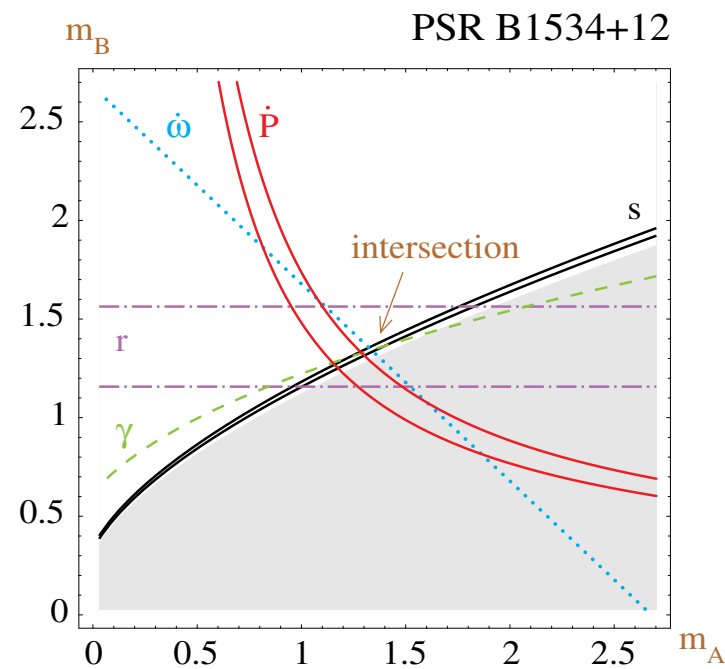
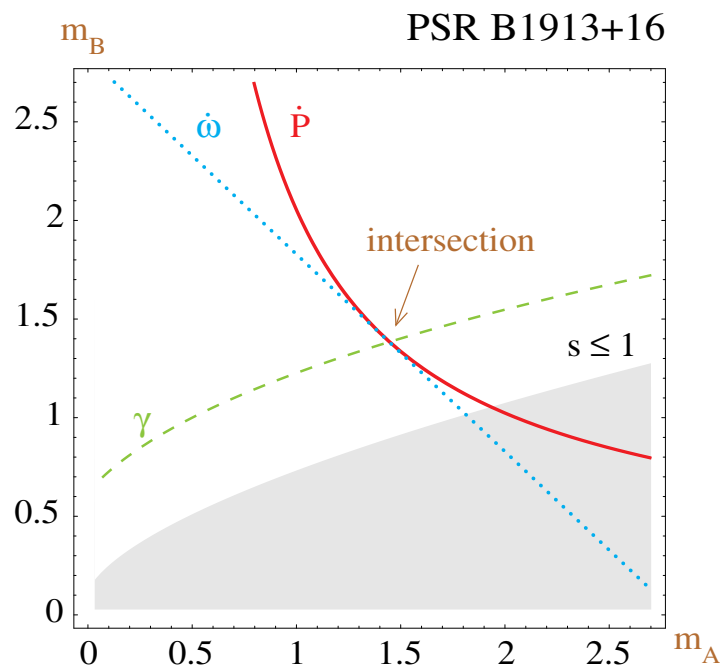


* Vertical axis ($\beta_0=0$): Brans-Dicke theory with $\alpha_0^2 = \frac{1}{2\omega_{BD}+3}$. In this case, solar-system tests are more constraining than the Hulse-Taylor binary pulsar PSR B1913+16.

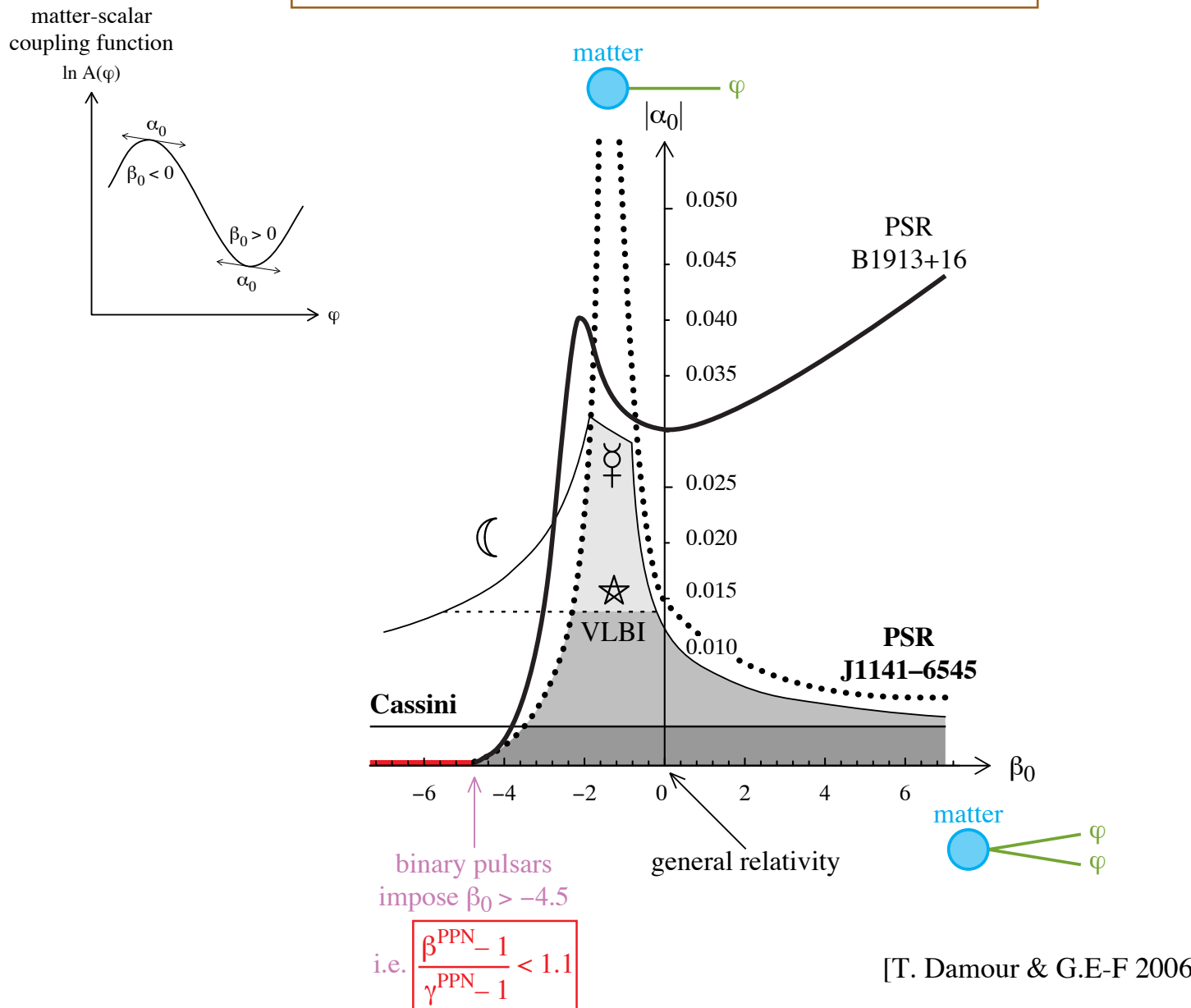
* Horizontal axis ($\alpha_0=0$): Theories which are perturbatively equivalent to G.R., and therefore undistinguishable from it in the weak-field conditions of the solar system. Binary pulsars rule out the models with $\beta_0 < -4.5$, because of the nonperturbative strong-field effects described in § A.7 above.

⇒ QUALITATIVE difference between solar-system & binary-pulsar tests!

The four accurately timed
binary pulsars in general relativity



Solar-system & best binary-pulsar constraints on scalar-tensor theories of gravity



Vertical axis ($\Phi_0 = 0$) : Jordan–Fierz–Brans–Dicke theory $\Phi_0^2 = \frac{1}{2 \Phi_{BD} + 3}$

Horizontal axis ($\Phi_0 = 0$) : perturbatively equivalent to G.R.

* Which of the 3 other (accurately timed) binary pulsars presented above is the most constraining? (53)

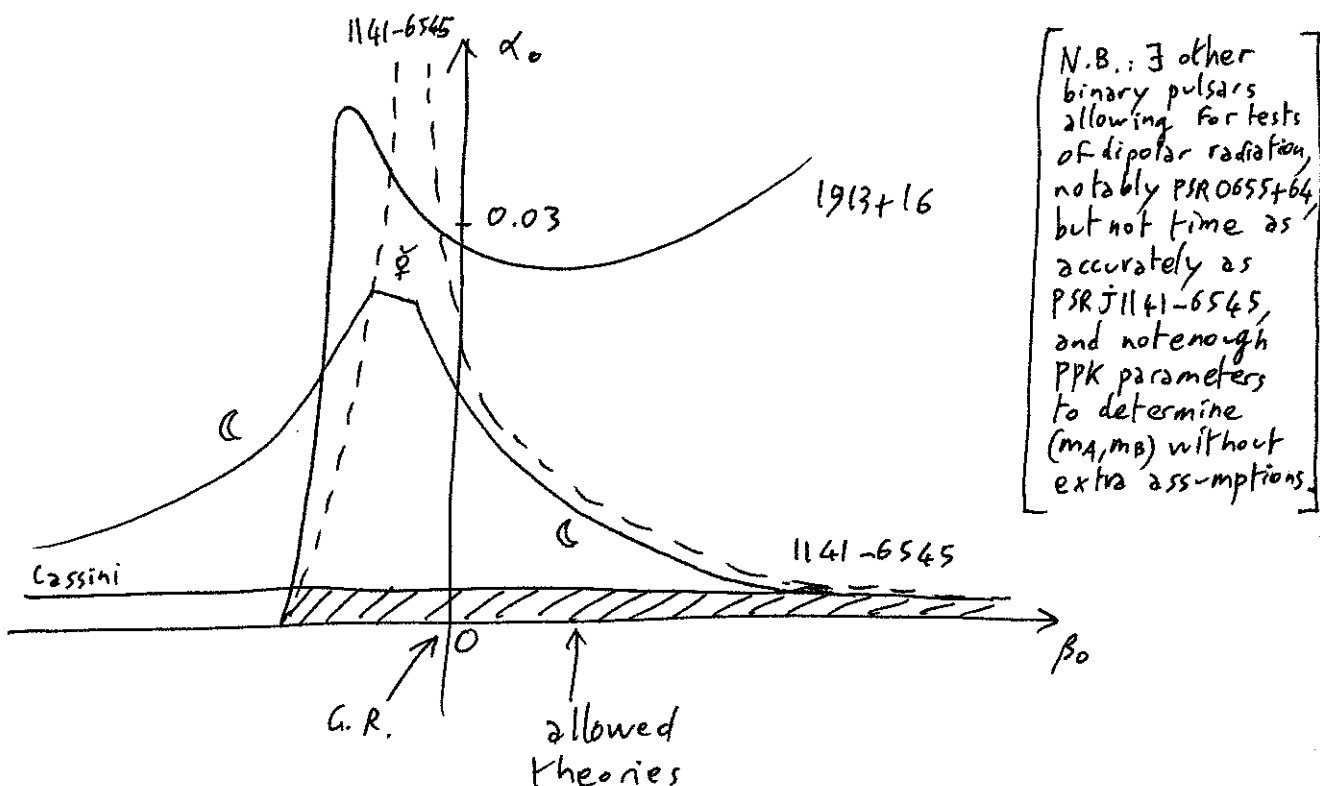
Paradoxically, this is the dissymmetric [PSR-White dwarf] system of § B.4, in spite of its rather large errors on \dot{P} . Indeed, its dissymmetry implies that it should emit a large amount of dipolar (scalar) waves

$$\propto (\alpha_A - \alpha_B)^2 \frac{1}{c^3}$$

may be $O(1)$

\approx do for a white dwarf (small binding energy)

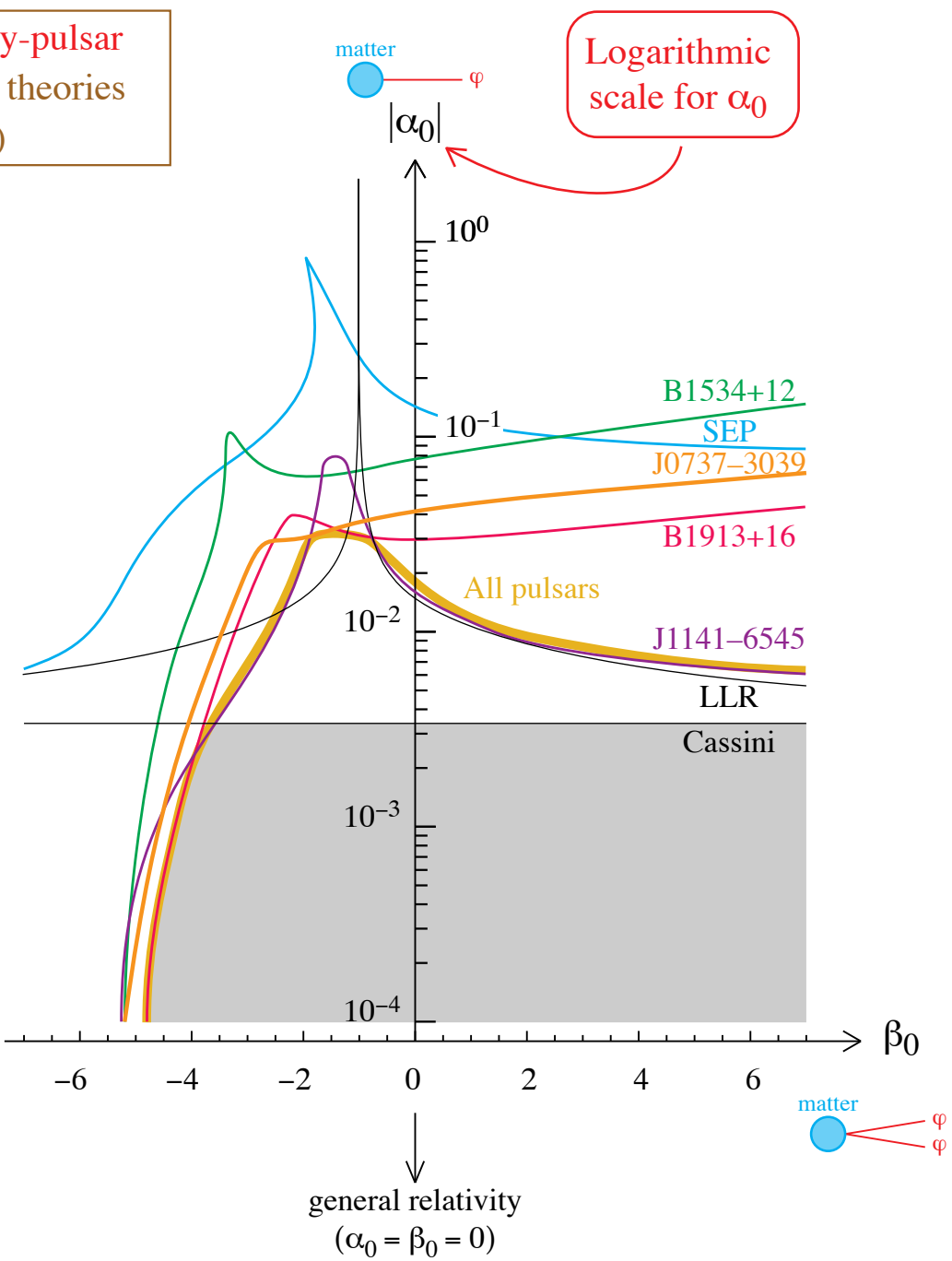
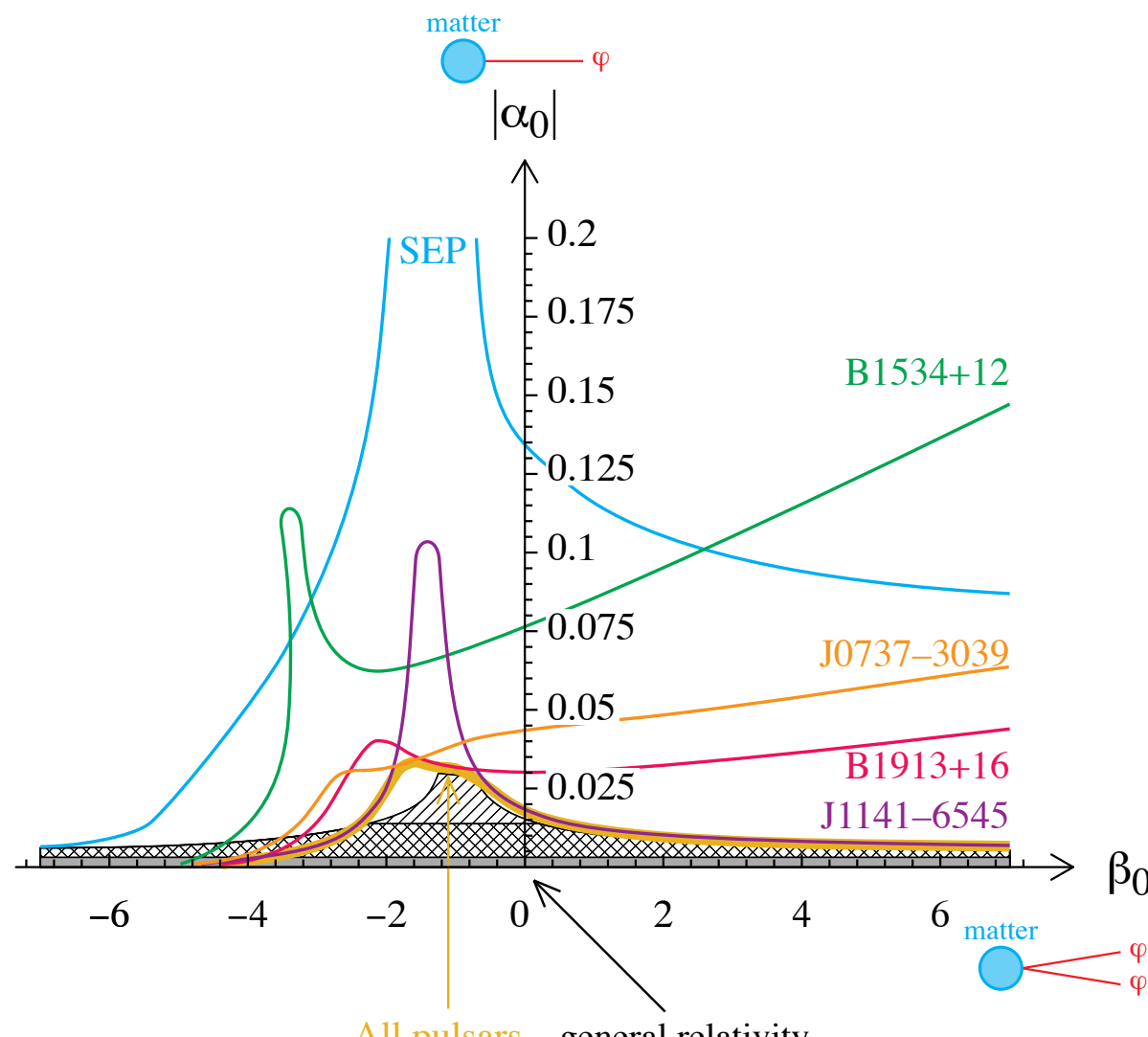
much larger than the G.R. $\frac{1}{c^5}$ quadrupole.



Not only more constraining than Hulse-Taylor (with low precision on \dot{P}), but also almost as constraining as solar system for $\beta_0 > 0$.

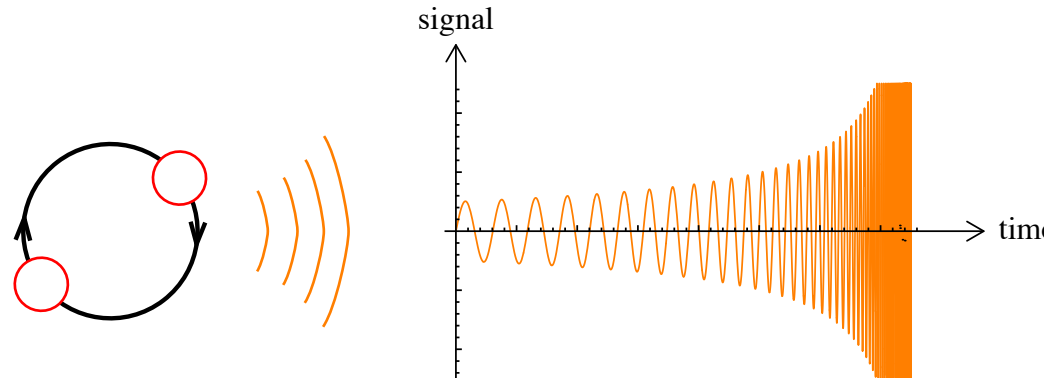
[Because $(\alpha_A - \alpha_0)^2 \sim (0 - \alpha_0)^2$ when $\beta_0 > 0$: "de-scalarization" effect
 ⇒ absence of dipolar radiation constrains again α_0 .]

**Solar-system and best binary-pulsar
constraints on tensor–scalar theories
(updated May 2006)**



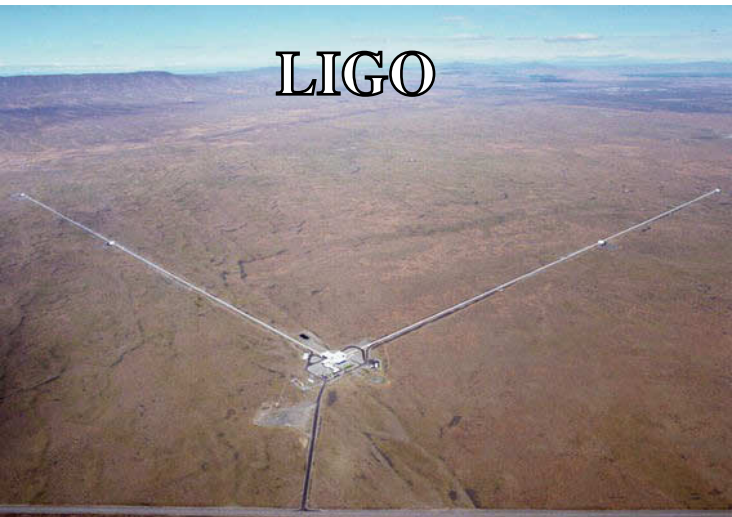
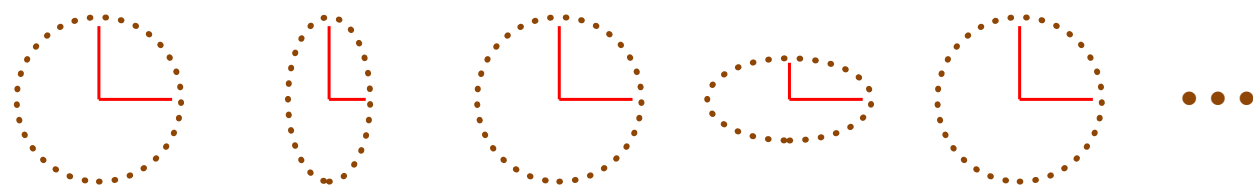
Gravitational wave antennas LIGO/VIRGO/LISA

- Signal emitted by an inspiralling binary system:



(depends on hundreds
of post-Newtonian
coefficients)

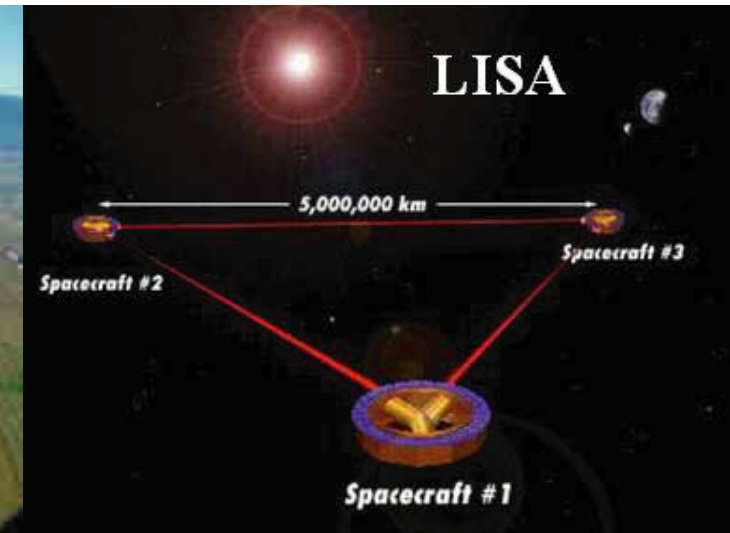
- Effect on a detector:



LIGO



VIRGO

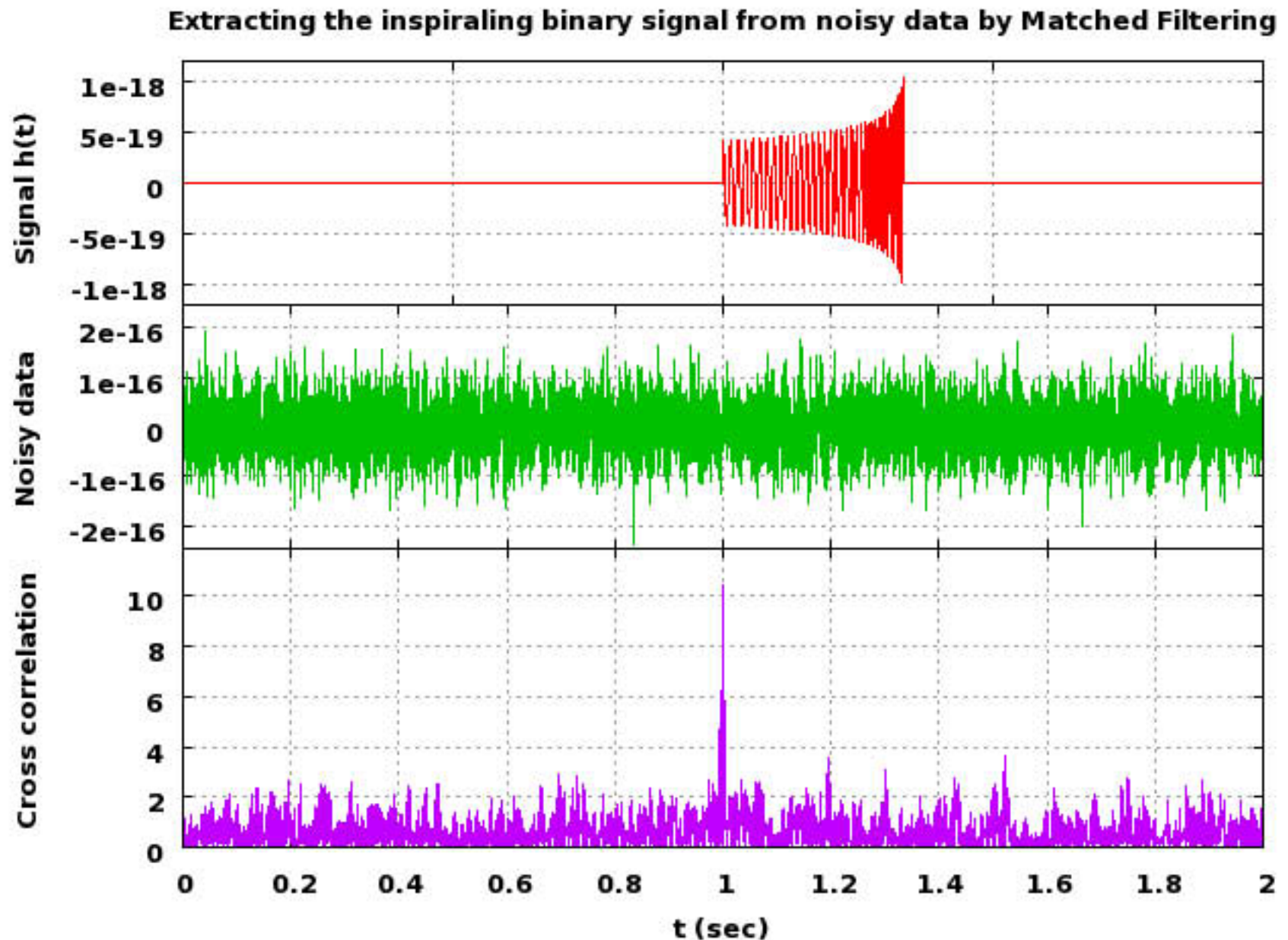
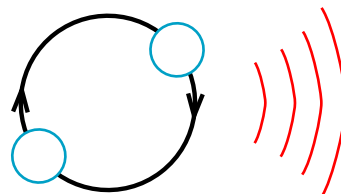


LISA

Gravitational wave antennas

LIGO/VIRGO/LISA

One needs accurate (3.5 PN) templates to extract the signal from the noise

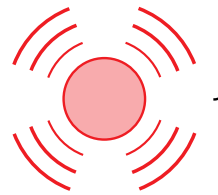


Gravitational waves in scalar-tensor gravity

$$\text{Energy flux} = \frac{\text{Quadrupole}}{c^5} + O\left(\frac{1}{c^7}\right) \quad \text{spin 2}$$

$$+ \frac{\text{Monopole}}{c} \left(\square + \frac{1}{c^2} \right)^2 + \frac{\text{Dipole}}{c^3} + \frac{\text{Quadrupole}}{c^5} + O\left(\frac{1}{c^7}\right) \quad \text{spin 0}$$

■ Collapsing star



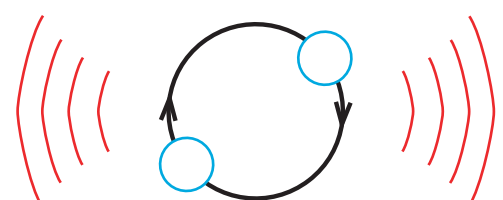
Energy flux
= (strong field)²
= Monopole/c
 \gg usual Quadrupole/c⁵

Factor $\square_0 = \frac{1}{\sqrt{2\square_{BD}+3}} \square \sqrt{\frac{1\square_{PPN}}{2}} < 0.003$

Detection
= (strong field) \square (weak field)
= too small for LIGO/VIRGO
[J. Novak's thesis, PRD **57**, 4789; **58**, 064019 (1998)]
and not in LISA's frequency band

■ Inspiralling binary

Even if no helicity-0 wave is detected, the time-evolution of the (helicity-2) chirp depends on the Energy flux = (strong field)²



\square A priori possible to detect indirectly the presence of \square :

If binary inspiral detected with GR templates
 \square bound on matter-scalar coupling strength

[matched-filter analysis: C.M. Will, Phys.Rev. D **50** (1994) 6058]

B.7: Comparison with LIGO/VIRGO and LISA

54

* Energy flux in scalar-tensor theories

$$= \frac{\text{Quadrupole}}{c^5} + O\left(\frac{1}{c^7}\right) \quad \text{spin } 2$$

$$+ \frac{\text{Monopole}}{c} \left(\dot{\phi} + \frac{1}{c^2} \right)^2 + \frac{\text{Dipole}}{c^3} + \frac{\text{Quadrupole}}{c^5} + O\left(\frac{1}{c^7}\right) \quad \text{spin } 0$$

\uparrow

$$\frac{d}{dt} (\text{scalar charge})$$

* Therefore, a collapsing star will emit a huge amount of monopolar waves



$$\begin{aligned} \text{Energy Flux} &= (\text{strong-Field})^2 \\ &= \text{Monopole}/c \\ &\gg \text{Usual quadrupole}/c^5 \end{aligned}$$

Detection of scalar waves?
 = (strong Field) \times (weak Field)
 ↑
 factor $|\alpha_0| < 0.003$
 = too small for LIGO/VIRGO
 [J. Novak's thesis, PRD 57 (1998) 4789]
 and not in LISA's frequency band

* Inspiralling binary: $\dot{\phi} = 0 \Rightarrow$ no helicity-0 wave of order $\frac{1}{c}$,
and helicity-0 waves anyway not detectable

BUT the time-evolution of the observed helicity-2 waves depend on the Energy Flux = (strong field)²

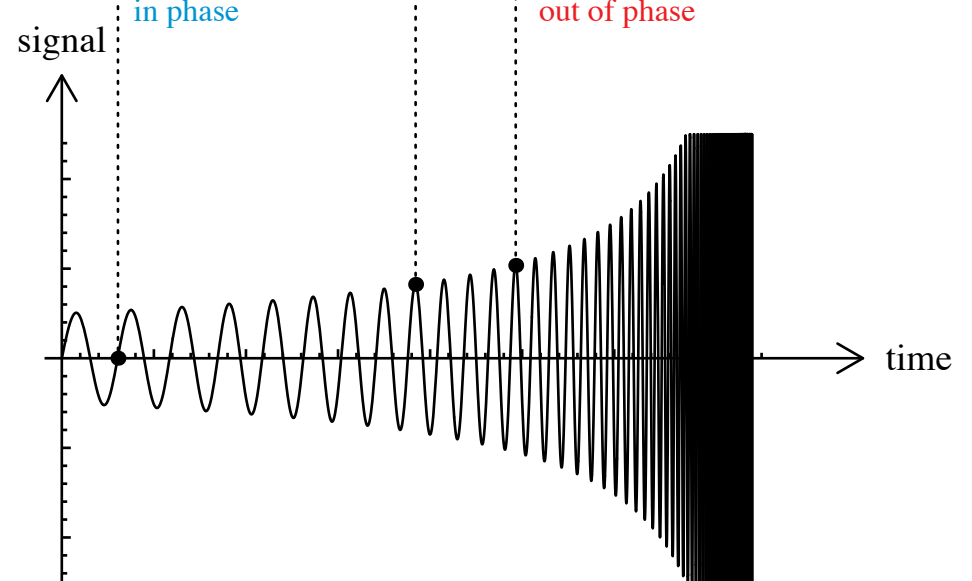
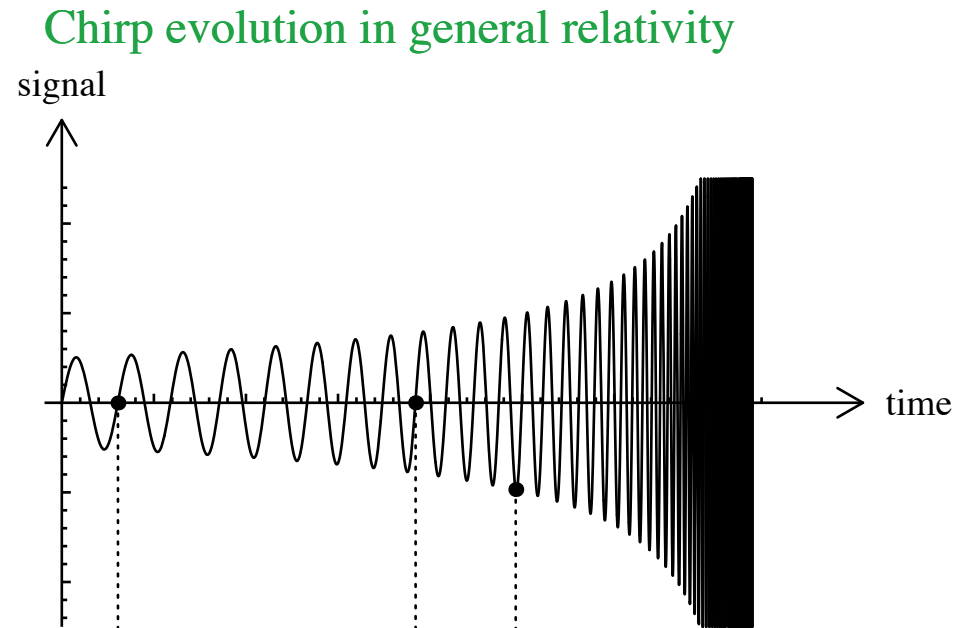
\Rightarrow a priori possible to detect indirectly the presence of ψ :

Matched-filter analysis [C. M. Will, Phys. Rev. D 50 (1994) 6058
 + Scharre & Will 2002 + Will & Yunes 2004
 + Berti, Buonanno & Will 2005]

If binary-inspiral detected with G.R. templates

\Rightarrow bounds on matter-scalar coupling strength

For an unknown mass of the system

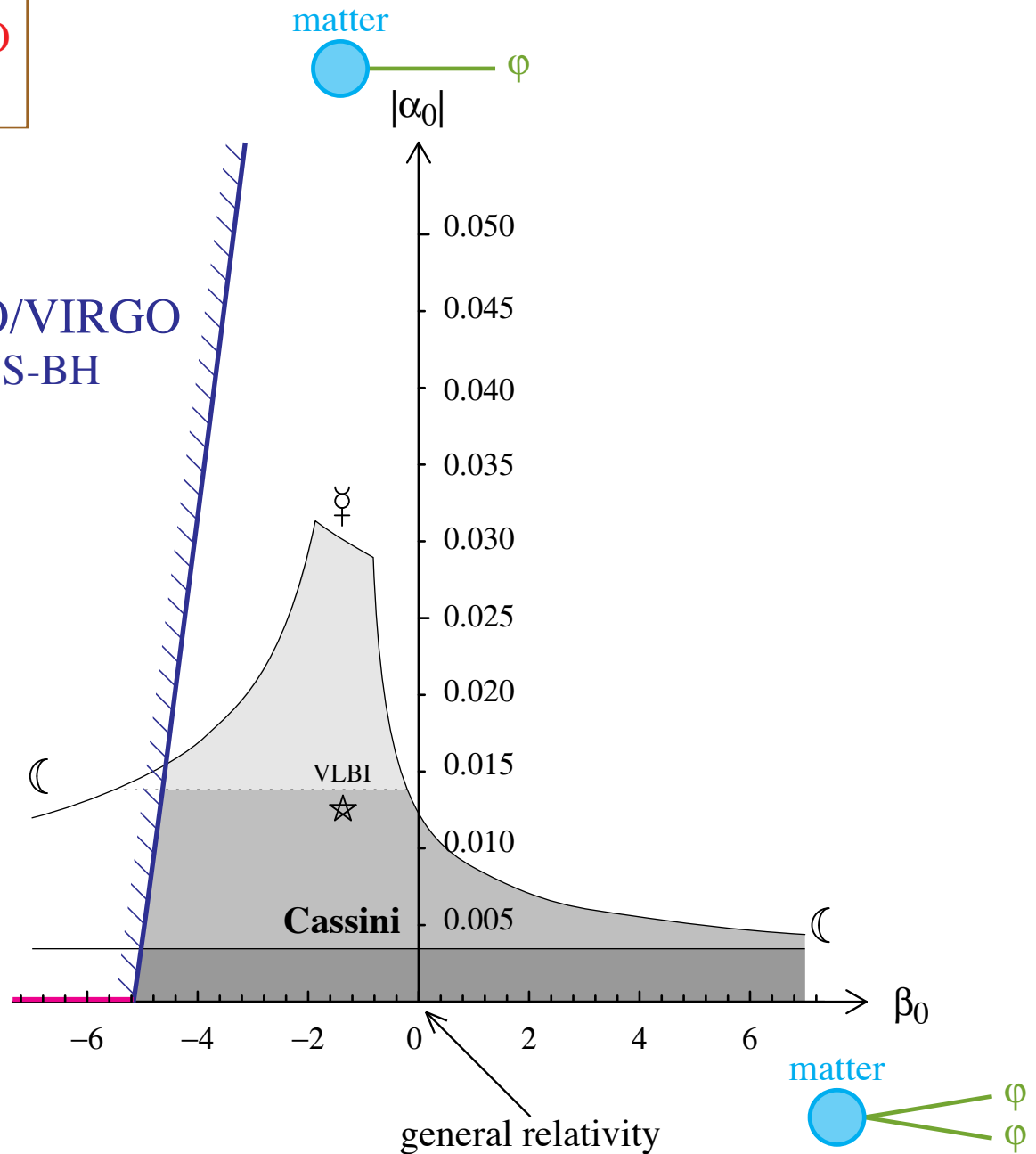


Chirp evolution in a tensor–scalar theory

Solar-system and possible LIGO/VIRGO constraints on scalar-tensor gravity

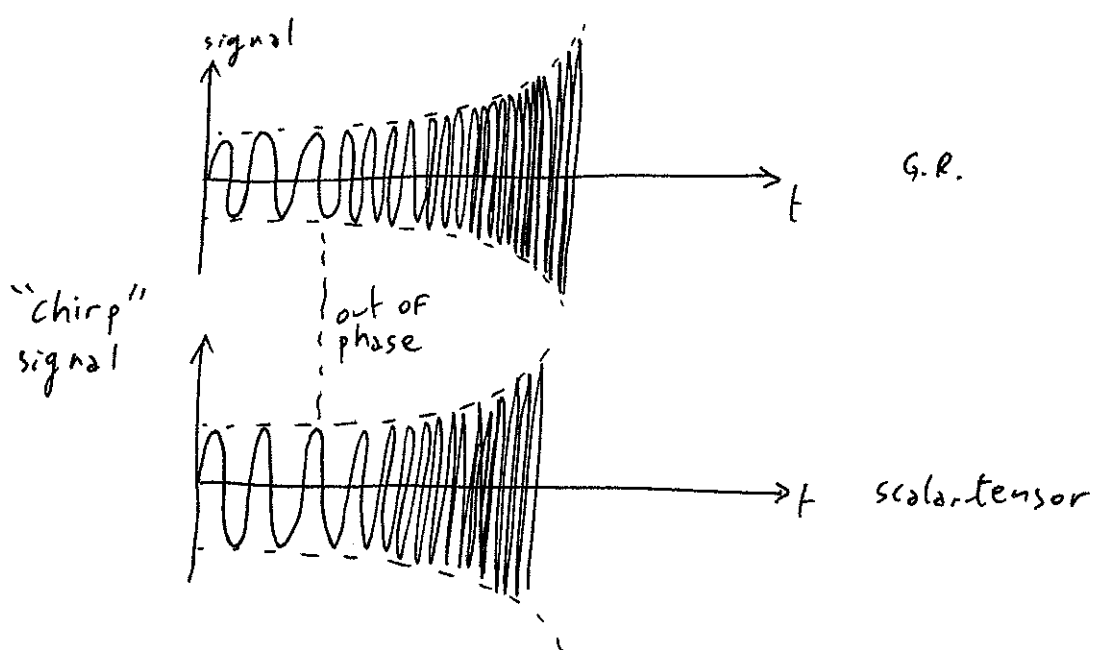
[Damour & GEF 1998]

LIGO/VIRGO
NS-BH

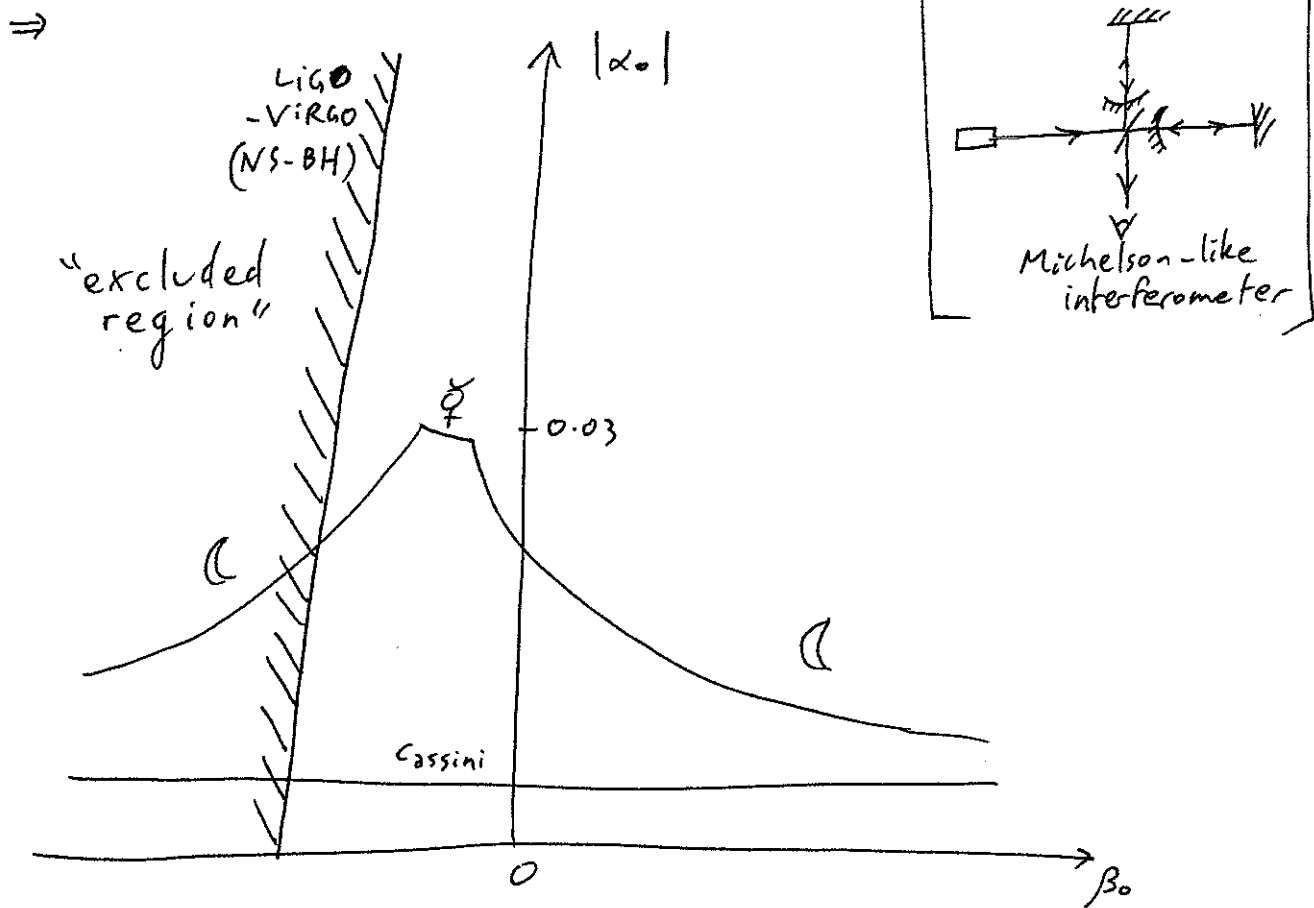


Vertical axis ($\beta_0 = 0$) : Jordan–Fierz–Brans–Dicke theory $\alpha_0^2 = \frac{1}{2 \omega_{\text{BD}} + 3}$
 Horizontal axis ($\alpha_0 = 0$) : perturbatively equivalent to G.R.

(55)

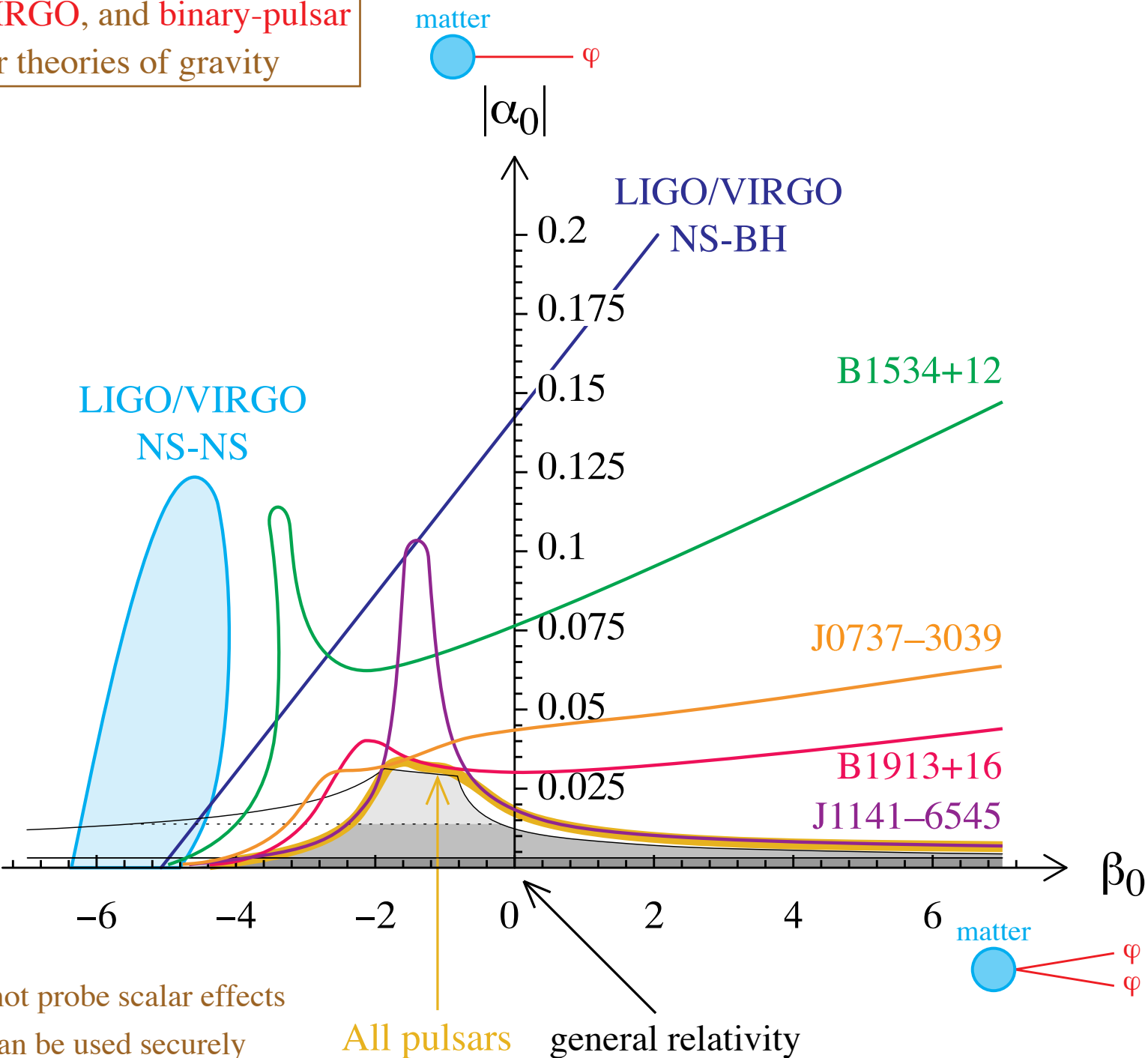


⇒ signal/Noise drops if 3 scalar field and "chirp" filtered with G.R. template.



"excluded region" = impossible to detect signal with G.R. template if (α_0, β_0) take those values.

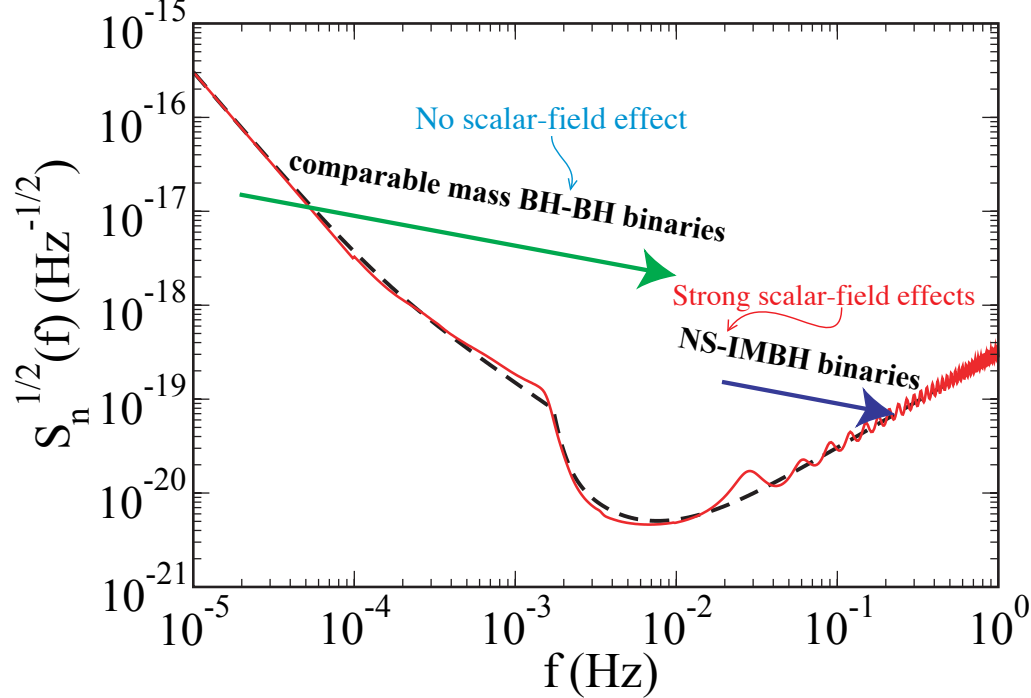
Solar-system, possible LIGO/VIRGO, and binary-pulsar
constraints on scalar-tensor theories of gravity



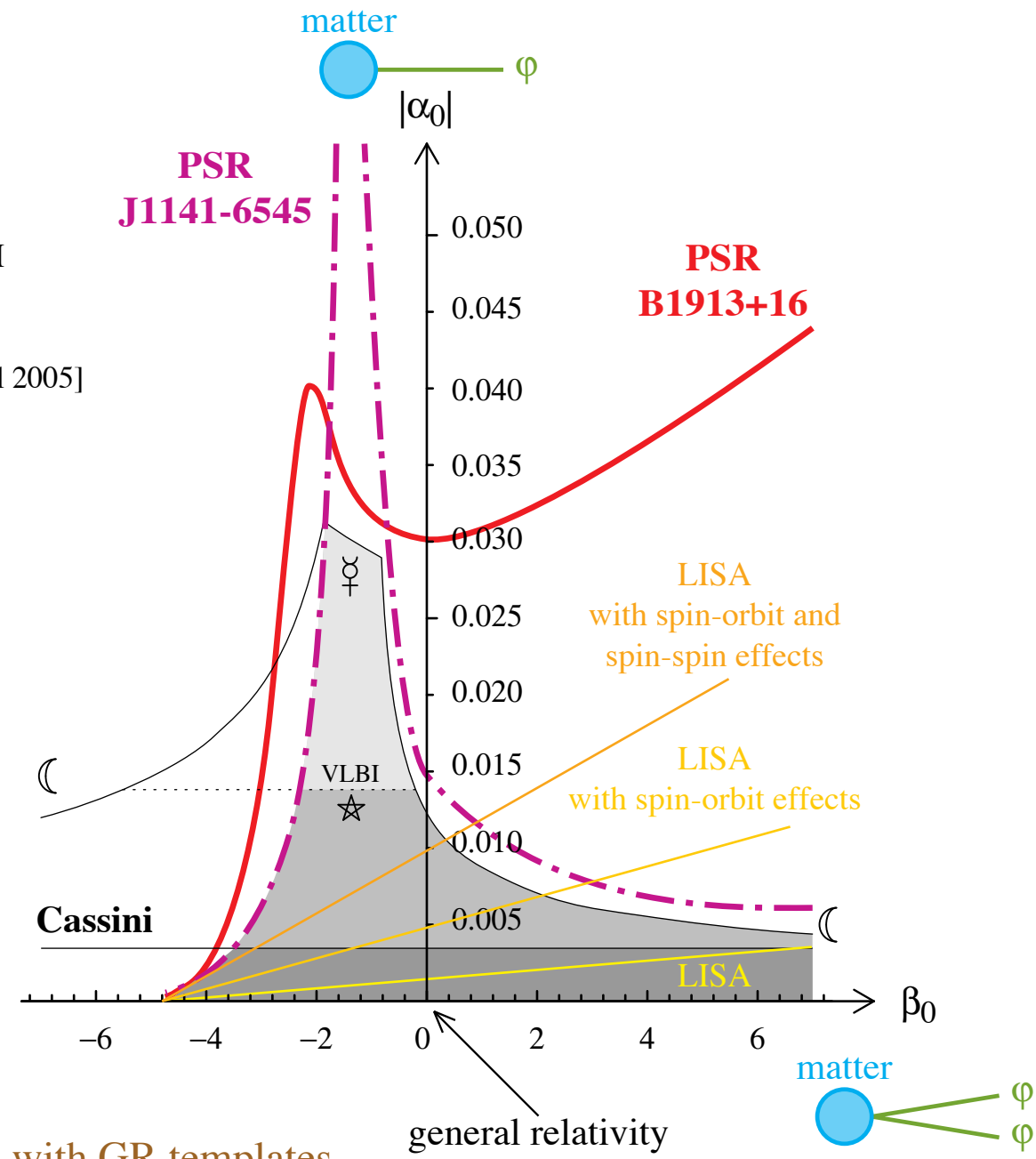
Possible LISA constraints on scalar-tensor theories of gravity

LISA will probe $|\alpha_0| \sim 1.5 \times 10^{-3}$ if $1.4 m_\odot$ NS – $1000 m_\odot$ BH observed with S/N = 10

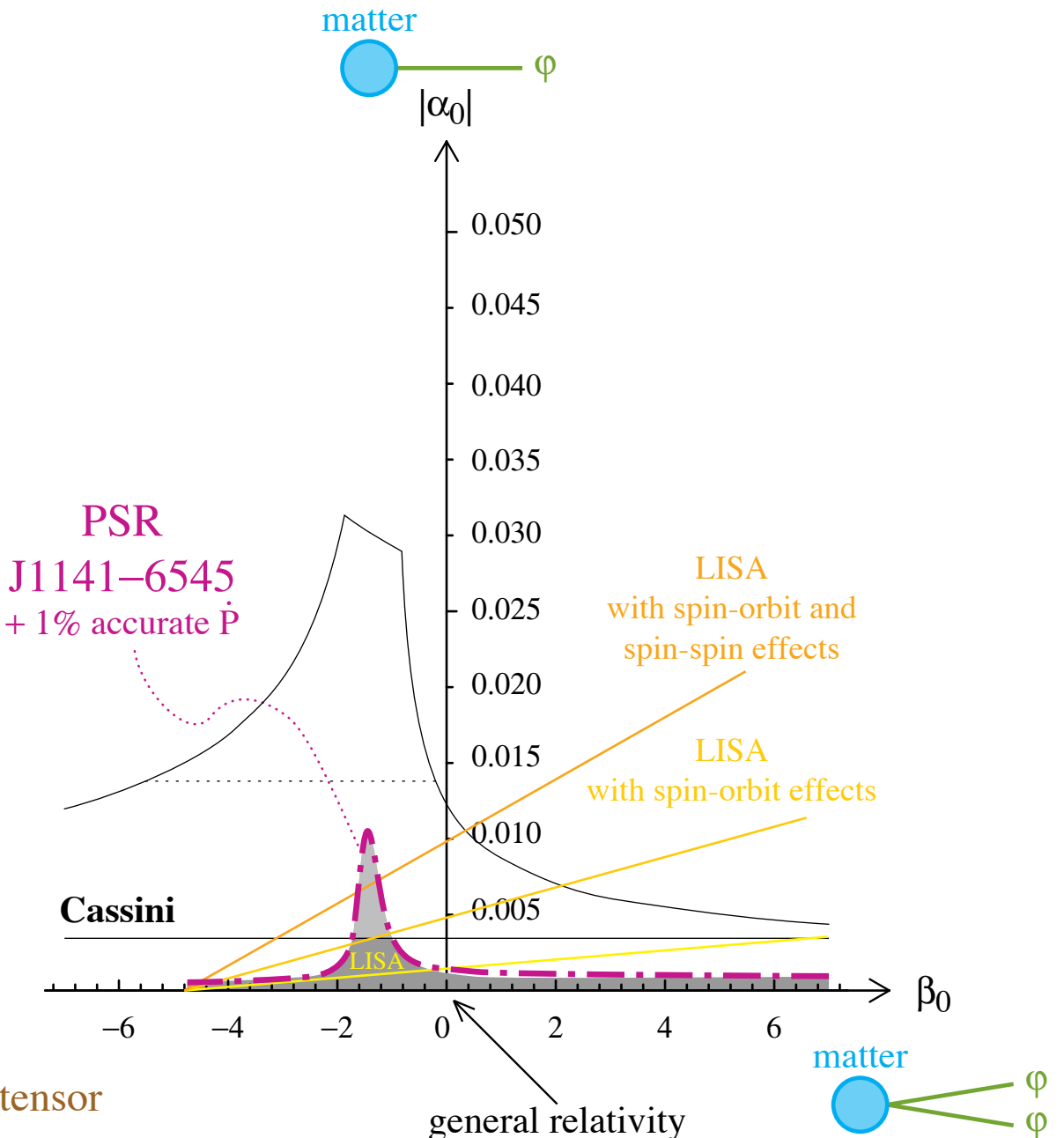
[Scharre & Will 2002; Will & Yunes 2004; Berti, Buonanno & Will 2005]



⇒ Tight constraints if detection of binary inspirals with GR templates
But if no detection, what would we conclude?



Future binary-pulsar constraints
on scalar-tensor theories of gravity



Binary pulsars will probably probe such scalar-tensor theories before LISA is launched

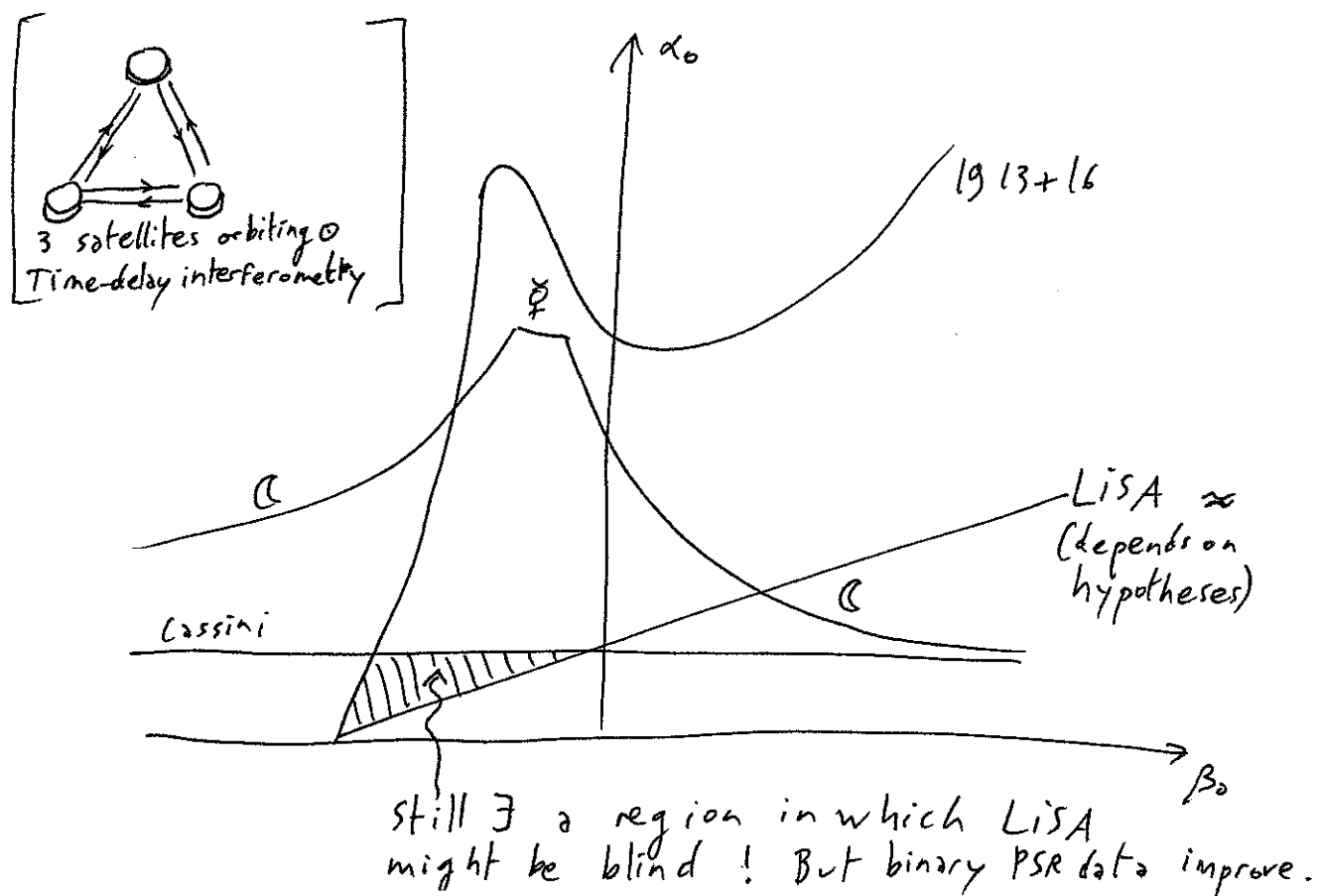
Good news: GR templates can be used securely

This would be a serious problem for LIGO/VIRGO:
 if no signal \rightarrow experimental noise too big?
 \rightarrow less sources than expected?
 \rightarrow or \exists scalar partner to graviton?

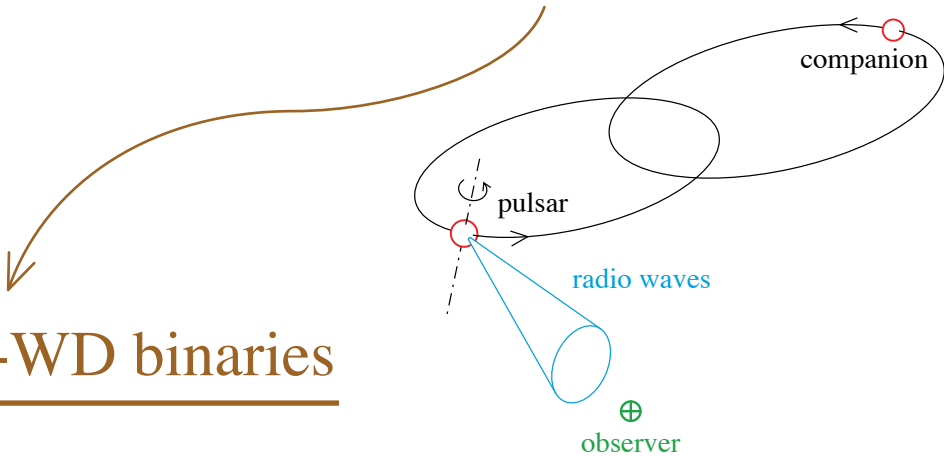
* Fortunately, binary pulsars already exclude this region of the theory-space.

Conclusion: one may trust G.R. wave templates for LIGO/VIRGO. Even if \exists scalar partner to graviton, binary pulsars already tell us that it is too weakly coupled to matter to modify significantly the waveforms.

* Same analysis for the LISA (space antenna)
 [Will + Scharre, Yunes, Berti & Buanzino 2002-2005]



- ~ 1600 known pulsars
- ~ 100 binary pulsars



Many NS-WD binaries

PSR J1141–6545 →
[Kaspi *et al.* 1999]

PSR J0407+1607
PSR J2016+1947
...

PSR J0751+1807 ⇒ $2.1 \text{ m}_\odot \text{ NS!}$
[Nice *et al.* 2005]

Precision tests of strong-field gravity

8 NS-NS binaries

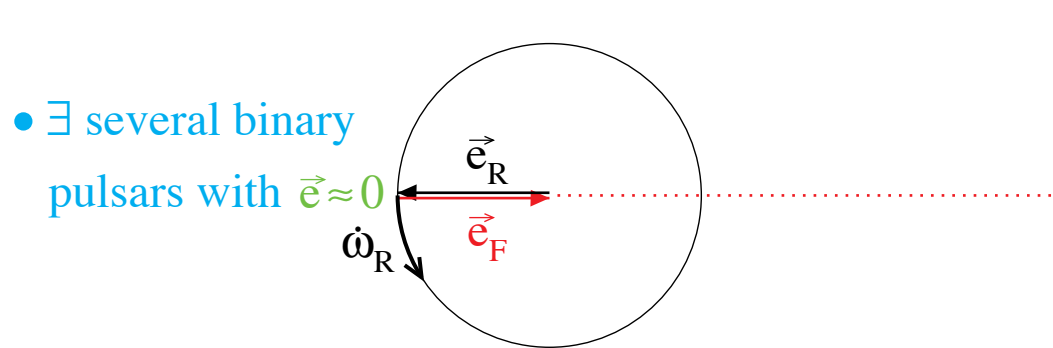
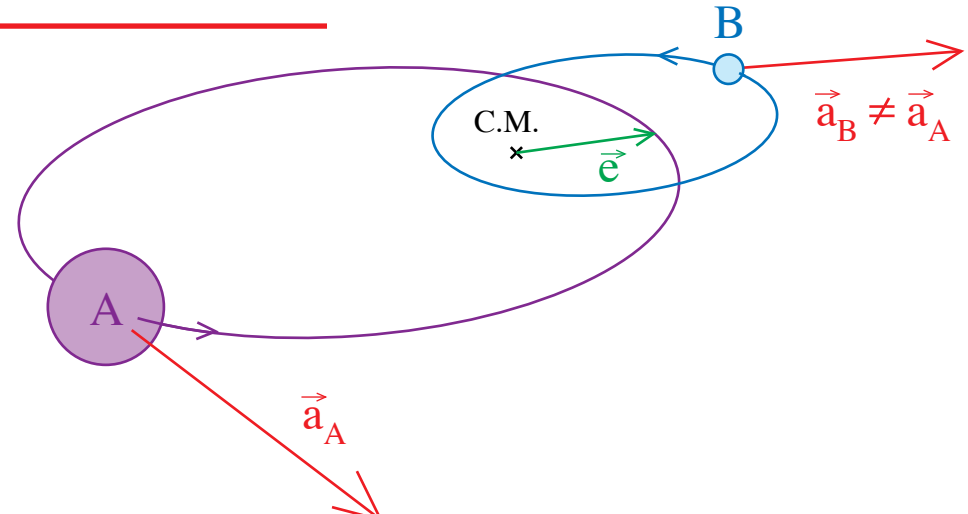
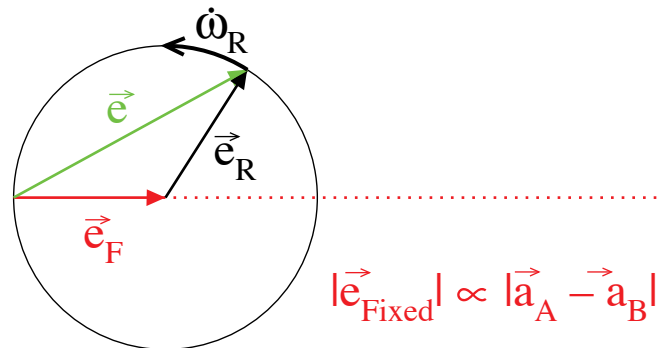
{ **PSR B1913+16** [Hulse-Taylor 1974]
PSR B1534+12 [Wolszczan 1991]
PSR J0737–3039 [Burgay *et al.* 2003]

PSR B2127+11C (in globular cluster)
PSR J1756–2251 [Faulkner *et al.* 2004]
PSR J1518+4904
PSR J1811–1736
PSR J1829+2456

PSR J1906+07 [Lorimer *et al.* 2005]
(maybe NS-WD?)

Tests of the “strong equivalence principle” and of preferred-frame effects

- The different accelerations (due to a third body or to their absolute velocity with respect to a preferred frame) induce a polarization of the periastron towards a precise direction



⇒ statistical argument to constrain PPN parameters

[Damour, Schäfer, GEF, Bell, Camilo, Wex, Stairs, ...]

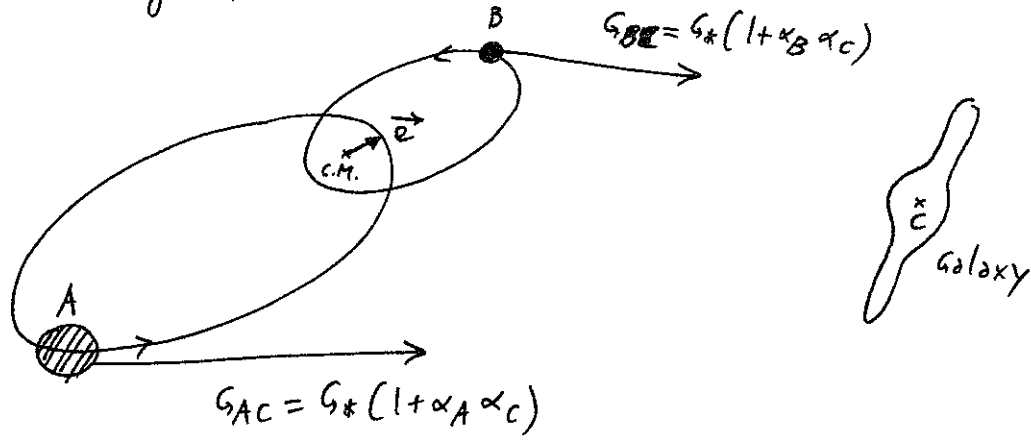
⇒ Constraints on PPN parameters

[Stairs *et al.* 2005]

- $|\alpha_1| < 1.4 \times 10^{-4}$ (\approx solar system bounds)
- $|\alpha_3| < 4 \times 10^{-20}$ (10^{12} tighter than sol. syst. !)
- $|1 - m_g/m_i| < 5.6 \times 10^{-3}$ for a neutron star

B.8: Null tests of symmetry principles

- * Tests of the strong equivalence principle (& preferred-frame effect)

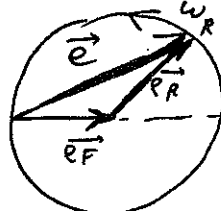


If $A = \text{neutron star} \Rightarrow \alpha_A = O(1)$ possible
 $B = \text{white dwarf} \Rightarrow \alpha_B \approx \alpha_0$

$\Rightarrow A \& B$ not attracted with same acceleration towards center of galaxy

* Using the technique of variation of constants illustrated in C. Will's lectures, one can prove that a difference between \vec{a}_A and \vec{a}_B causes a polarization of the orbit (cf. Nordtvedt's effect for the $\oplus C$ system attracted by \odot)

Eccentricity vector \vec{e} , norm e and directed from center of mass of system to periastron

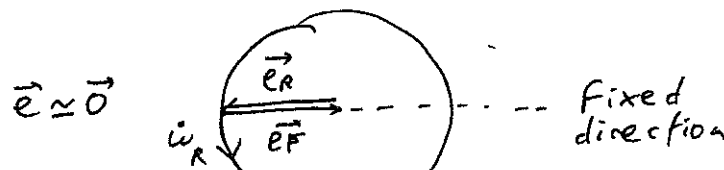


--- fixed direction

$$\vec{e}_{\text{observed}} = \vec{e}_F + \vec{e}_{RL}(1 - |\alpha_A - \alpha_B|)$$

rotating like in G.R. (cf. §)

* We know tens of NS-White dwarf systems with $e \approx 0$. Only possible explanation



[Damour, Schäfer, Gelfand, Bell, Camilo, Wex, + Stairs et al 2005] best analysis

$$\begin{aligned} |\alpha_1| &< 1.4 \times 10^{-4} \\ |\alpha_3| &< 4 \times 10^{-20} \\ |1 - mg/mi| &< 5.6 \times 10^{-3} \text{ for NS} \end{aligned}$$